DISCLAIMER

This report was prepared as an account of work sponsored by an agency of the United States Government. Neither the United States Government nor any agency thereof, nor any of their employees, makes any warranty, express or implied, or assumes any legal liability or responsibility for the accuracy, completeness, or usefulness of any information, apparatus, product, or process disclosed, or represents that its use would not infringe privately owned rights. Reference herein to any specific commercial product, process, or service by trade name, trademark, manufacturer, or otherwise does not necessarily constitute or imply its endorsement, recommendation, or favoring by the United States Government or any agency thereof. The views and opinions of authors expressed herein do not necessarily state or reflect those of the United States Government or any agency thereof. Reference herein to any social initiative (including but not limited to Diversity, Equity, and Inclusion (DEI); Community Benefits Plans (CBP); Justice 40; etc.) is made by the Author independent of any current requirement by the United States Government and does not constitute or imply endorsement, recommendation, or support by the United States Government or any agency thereof.

BNL-227572-2025-INRE

TCF - Sustainable Well Cement for Geothermal, Thermal Recovery, and Carbon Storage wells

T. Pyatina

January 2025

Interdisciplinary Science Department

Brookhaven National Laboratory

U.S. Department of Energy

USDOE Office of Energy Efficiency and Renewable Energy (EERE), Renewable Power Office. Geothermal Technologies Office

DISCLAIMER

Brookhaven National Laboratory

BNL-227572-2025-INRE

TCF – Sustainable Well Cement for Geothermal, Thermal Recovery, and Carbon Storage wells

July 2024

Tatiana Pyatina and Toshifumi Sugama

Project budget $500K – DOE $250K, Cost Share $250K

managed by Brookhaven Science Associates
on behalf of the U.S. Department of Energy

U.S. DEPARTMENT OF ENERGY

TABLE OF CONTENTS

1. INTRODUCTION

Primary cementing is the most important operation performed on a subterranean well. Cement, placed in the annulus between the casing and the formations serves as a hydraulic seal preventing fluids and gas migrations, protecting steel casing from corrosion and supporting the well structure. Poor cementing jobs can be directly responsible for wells not reaching their full capacity, casing corrosion, compromised well integrity and, in the worst-case scenarios, well collapse.

Geothermal, thermal recovery and carbon storage wells offer environments that are especially difficult for cements to survive while the required lifespan of these wells can be years. In these wells currently used cements cannot provide durable well integrity and new solutions are necessary. The necessity of stabilizing the electric grid, increasing its flexibility, and providing energy on demand will further expand the market of durable cement solutions for applications in high-temperature underground reservoir thermal energy storage wells (HT RTES).

The design challenges of special cement systems for such wells originate from chemistry limitations of currently used well cements, aggressive environments, temperature and repeated shock conditions associated with them, and very weak formations that are not uncommon in these wells. During the last 70 years the most common systems for thermal-well construction have been Ordinary Portland Cement (OPC) (absolute majority of the wells), silica-lime system and high-aluminum cement-containing formulations.

The major issues of calcium-silicate hydrates, that form during the hydration of OPC resulting in hardened material, are their poor chemical resistance to acids due to the calcium interactions with acid anions followed by its eventual dissolution, even in mild acids, such as carbonic acid from CO_2 dissolution, and inadequate bonding to the steel causing serious casing corrosion problems (Sugama & Pyatina, 2019). Performance of OPC-based cement may be significantly improved with organic additives; however, those are limited by their temperature stability.

An alternative to calcium-silicate cement was developed by BNL and commercialized by Halliburton as ThermaLock^{TM} cement. Calcium-aluminate-phosphate-based chemistry of the material allowed overcoming acid-resistance problems of OPC, especially in CO_2-rich geothermal environments. In 2012-2015, building upon this experience, BNL developed Thermal Shock Resistant Cement (TSRC) with the support of Geothermal Technology Office (GTO) of DOE. TSRC has high-temperature stable chemistry, superior properties of cement-metal casing bond and corrosion protection (4-times better than currently used OPC-based formulation), significantly outperforms common well-cements in thermal-shock tests, has self-healing properties, and like ThermaLock^{TM} is CO_2 resistant incorporating carbonate ions into stable hydrates (Gill et al., 2012).

Unlike OPC, the hydrated TSRC primarily consists of crystalline hydro-ceramic phase and amorphous Na_2O-aluminosilicate $(-Al_2O_3-SiO_2-)_n$- inorganic polymer phase withstanding a heating temperature of 600^{o}C. The main crystalline products of the blend depend on the curing temperature and time (Pyatina & Sugama, 2018). However, under all tested conditions in the temperature range between 100 and 300^{o}C these products have desirable properties and include natural minerals found under similar conditions in geothermal wells. The major crystalline products include low-temperature zeolites Linde A and gibbsite at 100^{o}C (katoite, as a minor phase), thomsonite, gismondine, katoite (sodalite, boehmite, analcime, dmisteinbergite, as minor products) at 200^{o}C, and dmisteinbergite/anorthite feldspar polymorphs, boehmite (hydroxysodalite/sodalite, muscovite and margarite) at 300^{o}C after a short curing time of one day. The fact that at higher temperatures the blend starts forming mica type minerals of muscovite and

margarite that are expected to be stable under aggressive conditions is very attractive for the long-term durability of HT geothermal wells.

This cement cured hydrothermally for 24 hours at 300ºC and then subjected to 5-cycles of thermal shock (one cycle: 600°C annealing for 24 hours followed by 25°C water quenching for 5 hours) did not show any noticeable change in compressive strength, while conventional well cement disintegrated and cracked in the first 3 cycles. The reason for this great thermal-shock resistance was formation of dense hydro-ceramic [hydroxysodalite, $Na_4Al_3Si_3O_{12}(OH)$] nano-scale crystals and amorphous aluminosilicate-backbone inorganic polymer with minimum or none CaO. Furthermore, TSRC modified with self-healing aid had outstanding strength-recovery properties under hydrothermal conditions at 300ºC recovering more than 100% of its original strength in 5 days under steam, alkaline carbonate or geothermal brine environments after compressive damage(Pyatina & Sugama, 2019a). Additionally, unlike OPC-based formulations, TSRC is CO_2-resistant because of the ability to sequester CO_2 into stable crystalline structures (Pyatina & Sugama, 2018). The most recent studies demonstrated a great ability of this cement sheath surrounding metal casing to withstand repeated thermal shocks (250ºC →25ºC water through the tube) for underground energy storage applications. OPC-based formulation failed in the first cycle in these tests(Pyatina & Sugama, 2019b).

Additionally, BNL work on field-applicable formulation showed acceptable base slurry rheological properties at mixing and a possibility of effectively controlling slurry pumping time with a retarder.

The TSRC formulation was further modified for applications in HT RTES to minimize energy losses through heat dissipation in upper parts of the well. This was achieved by designing hydrophobic thermally insulating lightweight thermal shock resistant formulation (TILTSRC). The very low thermal conductivity of below 0.4 W/m*K compared to the regular cement ~1 W/m*K thermal conductivity allowed decreasing heat losses by nearly 40% for the 1 km deep energy storage wells (Sugama & Pyatina, 2021).

This report covers work on increasing commercialization maturity of advanced BNL cementitious composites. The work was done by BNL in collaboration with industrial partners CUDD Energy Services, AltaRock, and HERO.

The introduction of any new cement product faces several technical and market barriers. These barriers include conservative industry nature, lack of durability criteria in cementing job evaluations, consistency, and availability of the TSRC blend components, logistical issues, material cost, availability of additives to modify properties of the slurries, and organization of commercial blend production.

Subterranean wells are expensive to construct, while a poor cementing job may result in a well-loss. Consequently, there is a general reluctance to use new materials for well-cementing. Laboratory tests can only partially reduce the risks and service companies prefer to rely on their experience. The risks are even higher for formulations incompatible with currently used OPC, requiring a separate set of equipment. This was the case with ThermaLock^{TM}, which is incompatible with OPC-based formulations. Like ThermaLock^{TM}, TSRC/TILTSRC is based on calcium-aluminate cement (CAC) that is not compatible with OPC. Accordingly, unless the blend is modified, a separate set of equipment is needed for mixing and pumping TSRC/TILTSRC, complicating well-construction logistics. This disadvantage could be partially removed by using the new grade of CAC, that has improved compatibility with OPC.

Another market barrier is the absence of cement durability requirement especially for oil and gas wells. Currently most cementing jobs are evaluated based on whether cement was successfully

placed into a well. However, in the case of HT geothermal wells development of a geothermal field is associated with power plant construction. As a result, the lifespan of at least several decades is expected from HT geothermal wells.
Since only short-term goals are commonly taken into consideration during well construction, materials cost is an important factor in choosing cementing formulations. Most advanced cements are more costly than a commonly used HT formulation of OPC/silica, which complicates their adaptation for geothermal well construction.
To overcome these barriers, it was decided to demonstrate the absolute necessity of using advanced cement formulations for HT geothermal well cementing and to work with a service company on a field applicable formulation that would meet geothermal wells and American Petroleum Institute (API) standards.
The importance of cement durability was demonstrated in well-exposure tests in harsh underground environments comparing advanced formulations against currently used ones. The most difficult conditions of high temperature and CO_2-rich environments were targeted. The current cementing solutions were expected to have severe limitations of durability under such conditions.
The API tests and optimization of the retardation of the alkali-activated CAC-based advanced formulation of TSRC was performed by CUDD Energy Services with the support of BNL.
Some additional work was done to investigate potential of blend modification to simplify field application logistics by increasing its compatibility with OPC-based formulations and to ensure consistency of the blend performance since fly ash that makes part of its composition is a waste product and its batch-to-batch variability can be expected.

2. EXPERIMENTAL WORK

2.1. Exposure of cement samples in HT geothermal well.

Disclaimer: A part of this work was done in the frame of TEST-Cem project under the umbrella of GEOTHERMICA (Pyatina et al., 2024).
BNL partnership with AltaRock and HERO offered a unique opportunity of cement samples exposure in a real HT geothermal well. Laboratory evaluations of most well cements are conducted after their hydrothermal synthesis at HT and high pressure (HP) conditions followed by room-temperature analyses. Reproduction of geothermal well environments and long-term tests are problematic. As a result, field exposure of experimental cements under relevant geothermal conditions is an attractive alternative to laboratory testing. To take full advantage of this unique opportunity multiple cement formulations including those under the development for super-critical geothermal wells were tested during the exposure tests. Persistence of their performance was compared against the control of OPC/silica blend commonly used for cementing geothermal wells. In addition to the reference of OPC/silica with different ratios between OPC and silica flour, a lightweight blend of OPC/silica/Fly ash F (FAF), Calcium Aluminate Cement (CAC)/silica blends with different grades of CAC, calcium phosphate (CAP) cement blends with different grades of CAC and metakaolin (MK), TSRC, and a Ca-free gibbsite-based cement were field tested in a deep geothermal Newberry well for 3 and 9 months. The well-exposed samples were analyzed for the changes in their mechanical properties, water-fillable porosity, and phase compositions to understand stability and degradation of cements with different chemistries under HTHP geothermal conditions.

2.1.1. Well conditions, materials, samples preparation, exposure tools.

The exposure tests were performed in one of the deep Newberry wells (55-29) using made-for-purpose stainless steel cement sample holders (baskets). The baskets were lowered to the bottom of the well in July 2022 and retrieved in October 2022 for the 3-month exposure and lowered in October 2022 and retrieved in July 2023 for the 9-month exposure tests. The chapters below describe the well conditions, the baskets, and cement formulations tested in the well.

2.1.1.1. Well conditions

Figure 1 shows temperature (T) and pressure (P) profiles of the exposure well. T/P at the bottom of the well where the sample baskets remained is circled. The temperature at the bottom reached ~325-350ºC. The information on the pressure at the bottom of the well was not available, the pressure at the depth of about 1.6 km was nearly 2000 psi. If a constant pressure gradient is assumed between 1.6 and 3.0 km the bottom hole pressure can be estimated to be ~3700 psi.
The chemistry of the well environment at this location was not known. Trenton Cladouhos (former senior Vice President at AltaRock) provided the following information concerning possible CO_2 presence in the well environment:
"*In 2011, there was a 2000 psi gas cap that needed to be bled off for a few hours prior to logging. It was not sampled, but it was assumed to be CO_2.*
The gas flow did drop to near-zero, so we assumed that the CO_2 flux to the well was low and takes a long time to build up.
In 2012, there was a 600 psi gas cap that needed to be bled off prior to stimulation. It was not sampled, but it was assumed to be CO_2.
In 2013, there was a 600 psi gas cap that needed to be bled off prior to logging. It was sampled, and was mostly N_2, because an airlift was attempted in 2012 and that air was still downhole.
In 2022, October, there was a 1200 psi gas cap that was released in an attempt to flow-test the well. It was not sampled, but it was assumed to be CO_2. We also assume that this gas was produced by the decomposition of organic-based thermally degradable diverter.
In 2023, last week, Geoff checked the pressure gauge and there is no pressure at the well-head, so no expected gas cap. There was no longer any diverter to degrade and connectivity of previous CO_2 source is no longer there due to 2014 stimulation activity or 7 months was not enough time to build up a noticeable gas cap."
This suggests that although CO_2 could be present in the well, the concentration of the gas was unlikely to be high.
On the other hand, the Geochemical Analysis from Flow Testing of Well 55-29 by Geologica provided by Trenton, performed in 2008 reported that a non-condensable gas, identified as being >99% CO_2, was coming from a geological source (hydrothermal or magmatic). The total carbonates concentration measured at 2 different locations in well fluids was 296 and 1930 mg/kg. If this information is correct and the source of CO_2 was geological, high concentrations of CO_2 in the well could be expected.

2.1.1.2. Materials and samples preparation

Eleven different cement formulations were prepared and exposed in the well for 3 months (Table 1), 12 formulations were exposed in the second 9-month exposure test.

Calcium aluminate cements (CAC), Secar #80-, Secar #71-, Secar #50-, and Class G OPC, were used in this study. All CACs were supplied by Imerys, while Trabits group provided Dyckerhoff Class G, well cement. The X-ray powder diffraction (XRD) data showed that the crystalline compounds of #80 CAC were the following three principal phases, calcium monoaluminate ($CaO.Al_2O_3$, CA), calcium dialuminate ($CaO.2Al_2O_3$, CA_2) and corundum (α-Al_2O_3); #50 CAC had CA as its dominant phase, coexisting with gehlenite [$Ca_2Al(Al,Si)_2O_7$] and corundum as the secondary components. The Class G consisted of hatrurite ($3CaO.SiO_2$) as a major, and brownmillerite ($4CaO.Al_2O_3.Fe_2O_3$), basanite ($CaSO_4.1/2H_2O$) and periclase (MgO) as minor phases for the former cement. Among the cement-forming constituents, SMS (Na_2SiO_3), alkali-activating powder, of 93% purity, with the particles' size of 0.23- to 0.85-mm, trade named "MetsoBeads 2048," was supplied by the PQ Corporation. It had a 50.5/46.6 Na_2O/SiO_2 weight ratio. Sodium hexa-meta-phosphate (SHMP) [$(NaPO_3)_6$, 60-70% P_2O_5] with 200 mesh granular obtained from Sigma-Aldrich was used as a cement-building component of calcium-phosphate cements. Silica flour was supplied by Cudd Energy Services. The metakaolin ($Al_4Si_2O_{10}$), was obtained from Imerys. FAF was supplied by Boral Material Technologies. The XRD analysis of FAF showed that it included three major crystalline phases, quartz (SiO_2), mullite ($3Al_2O_3.2SiO_2$), and hematite (Fe_2O_3). The fly ash cenospheres were supplied by Imerys under the commercial name of MetaStar 501HP. For TILTSRC formulation and chemicals please see (Sugama & Pyatina, 2021). TILTSRC designed for lower temperatures (up to 250°C), where heat losses would be prevented due to the cement insolating nature, than those in the well of the field exposure tests (up to 350°C) was tested in 3-month exposure tests, but not in 9-month exposures.

Aluminum hydroxide, an EMPLURA® hydragillite powder with a bulk density of ~90 g/100 mL and particle size < 150 μm for 90% of the material, was obtained from Sigma Aldrich. Zirconium (IV) hydroxide as hydrous zirconium oxide, $ZrO_2.nH_2O$ (Zr), was also obtained from Sigma Aldrich.

The formulations exposed for 9 months between October 2022 and July 2023 were modified with 5% by weight of dry blend micro carbon fibers (MCF, AGM-94) derived from a polyacrylonitrile precursor, supplied by Asbury Graphite Mills, Inc. They were 7-9 microns in diameter and 100-200 microns in length. These fibers are stable at dry heat temperatures of ~600°C. They were used to increase the toughness of the tested composites and to evaluate their stability under the well conditions. Cement slurries were mixed at different water-to-cement ratios to obtain similar self-leveling properties.

All samples were autoclaved for a day at 300°C before shipment to the well side for exposure tests.

Table 1. Formulations exposed in the Newberry well for 3 months.

Formulation	Composition
1. CSH-60/40	OPC (60%)/silica flour (40%)
2. TSRC	TSRC
3. CAP#71/FAF	CAC #71 (70%)/FAF (30%)/6% bwob SHMP
4. CAP#71/Silica/MK	CAC #71 (60%)/silica flour (30%)/MK (10%)/6% bwob SHMP
5. CAP#50/FAF	CAC #50 (70%)/FAF (30%)/6% bwob SHMP

6. NAS-M1	Gibbsite (60%)/silica flour (40%)/10% bwob zirconium hydroxide/5% bwob SMS
7. #71/Silica	CAC#71 (60%)/silica flour (40%)
8. #71/Silica/MK	CAC#71 (60%)/silica flour (30%)/MK (10%)
9. #80/Silica	CAC#80 (60%)/silica flour (40%)
10. CSH-70/30	OPC (60%)/silica flour (40%)
11. CSH/FAF/Silica	OPC (40%)/FAF (30%)/silica flour (30%)
12. TILL TSRC-PMHS	Lightweight TSRC with fly ash cenospheres treated with PMHS (Sugama & Pyatina, 2021)

Table 2. Formulations exposed in the Newberry well for 9 months.

Formulation	Composition
1. CSH-60/40/MCF	OPC (60%)/ silica flour (40%)/5% by weight of blend (bwob) MCF
2. TSRC/MCF	TSRC/5% bwob MCF
3. CAP#50/FAF/MCF	CAC #50 (70%)/FAF (30%)/6% bwob SHMP/5% bwob MCF
4. CAP#71/FAF/MCF	CAC #71 (70%)/FAF (30%)/6% bwob SHMP/ 5% bwob MCF
5. CAP#71/Silica/MK/MCF	CAC #71 (60%)/silica flour (30%)/MK (10%)/6% bwob SHMP/ 5% bwob MCF
6. #71/Silica/MCF	CAC#71 (60%)/silica flour (40%)/ 5% bwob MCF
7. #80/Silica/MCF	CAC#80 (60%)/silica flour (40%)/ 5% bwob MCF
8. CAP#71/Silica/MK-2/MCF	CAC #71 (60%)/silica flour (25%)/MK (15%)/6% bwob SHMP/ 5% bwob MCF
9. NAS/CAC/silica	Gibbsite (50%)/CAC#80 (10%)/silica flour (40%)/5% bwob SMS
10. NAS/CAC/silica/MCF	Gibbsite (50%)/CAC#80 (10%)/silica flour (40%)/5% bwob SMS/5% bwob MCF
11. NAS/MCF	Gibbsite (60%)/silica flour (40%)/5% bwob SMS/5% bwob MCF
12. NAS/Zr/MCF	Gibbsite (60%)/silica flour (40%)/10% bwob zirconium hydroxide/5% bwob SMS/5% bwob MCF

2.1.1.3. Exposure tools

Exposure tools (baskets) were fabricated from stainless steel to host cylindrical samples of 40x20 mm size (Figure 2). They had open slots for samples exposure to the well environment. Three baskets could be fitted on top of each other and removed together or separately from the well. The baskets were designed in collaboration with - and fabricated by Renegade Services.
The baskets were loaded with precured samples and deployed in the well on a wireline, detached from the wireline, and left at the bottom of the well. The retrieval of the baskets 3 and 9 months later was successful, and all the samples were recovered in good shapes without any visible damage

(Figure 3). Similarly, samples exposed for 9 months in the well did not show any visible damage (not shown).

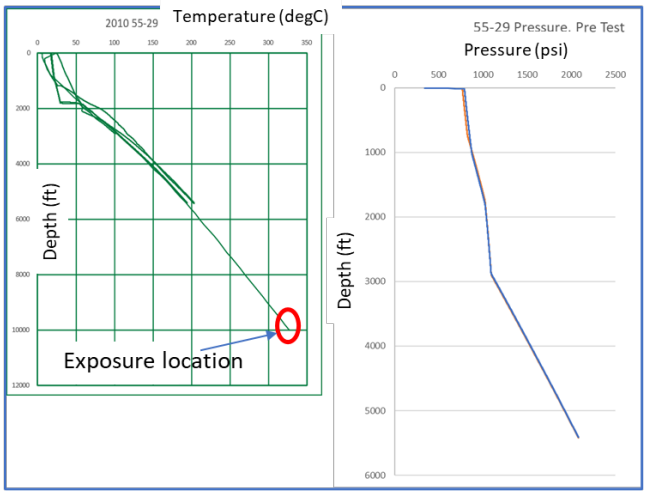

Figure 1: Temperature and pressure data for the exposure well with the exposure location at the bottom of the well shown by the red circle. The data show that the exposure temperature was above 300ºC (~350ºC) and pressure ~3700 psi.

Figure 2: Photographs of the exposure basket (middle and right) and a basket with two cement samples (left).

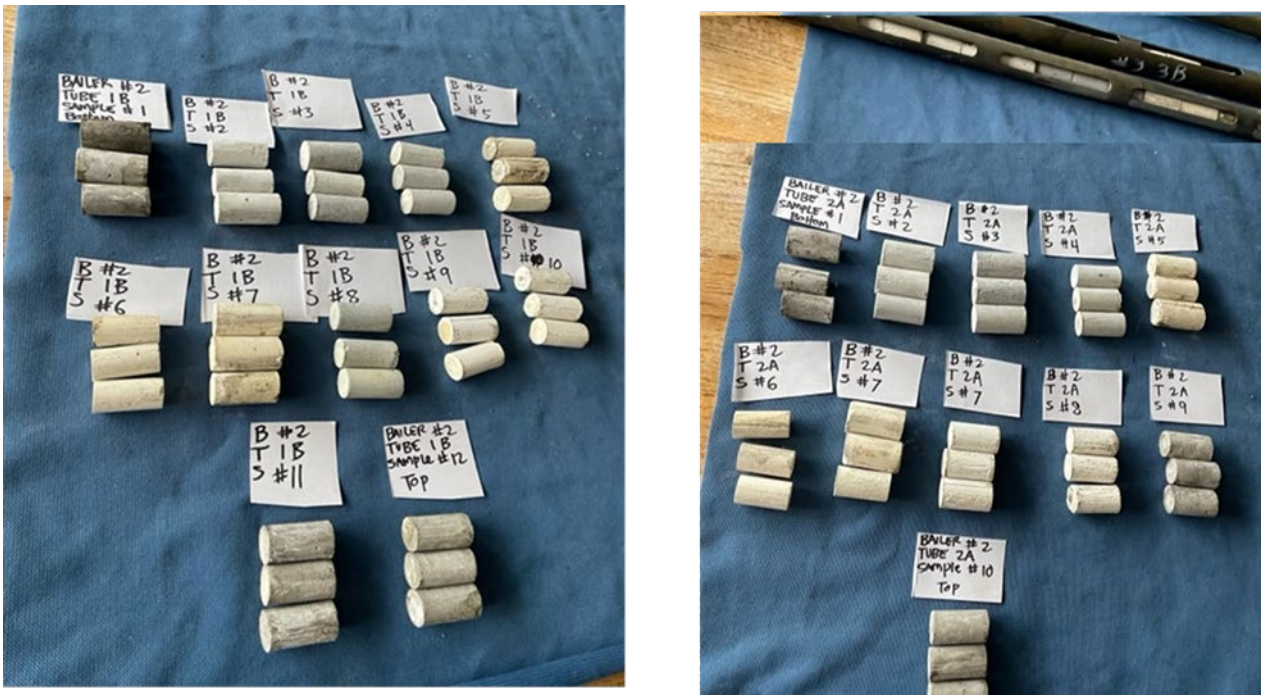

Figure 3: Photographs of the samples after the 3-month exposure in the Newberry well.

2.1.2. Samples analyses

2.1.2.1.Mechanical properties and porosity.

Mechanical and physical properties of 11 exposed formulations were analyzed after the 3 months of exposure. These included water-fillable porosity, unconfined compressive strength, Young's modulus (YM), and compressive toughness. The results are shown in Table 3. All the tested formulations had acceptable strength of more than 1000 psi (7MPa). CSH-1 (OPC/SiO_2, 60/40) and calcium phosphate cement with CAC#71 had the highest strength and the lowest porosity (4300 psi, 34% and 4600 psi, 36% respectively). High YM accompanied the high strength of the phosphate cement formulation (630 kpsi) placing this blend into the region of brittle fracture failure (Sugama & Pyatina, 2019a). This corresponded to a low toughness value of 0.21 N*mm/mm^3. The YM of the OPC formulation (460 kpsi was in the desirable moderate failure range where cement is neither soft nor brittle. Relatively toughness (0.53 N*mm/mm^3) of this cement formulation suggested a good balance between strength and ductility. HT OPC formulation with higher silica content of 40% performed noticeably better than that with 30% silica for all measured parameters. Of all OPC-based formulations, the formulation with SiO_2 partially replaced by FAF, was the lowest in strength and the highest in porosity (#11). It also had a low YM value of 190 kpsi (borderline soft failure). The toughness (0.41 N*mm/mm^3) of that formulation was reasonably high because of its high ductility. This formulation was a lightweight one (~1700 kg/m^3) unlike the rest of the cements, which can explain its lower mechanical properties.

Two cement formulations that exhibited an outstanding combination of strength and ductility were TSRC (toughness of 0.61 N*mm/mm^3) and gibbsite cement (NAS-M1, toughness of 0.73 N*mm/mm^3). Strength, toughness, and YM decreased for CAC #71/SiO_2 formulation after the 3-month exposure.

TILTSRC hydrophobic formulation (#12) designed for the upper temperature limit of 250°C survived the exposure with excellent mechanical properties and low porosity. Because the exposure temperature exceeded its specifications the hydrophobic property of the cement was lost. Nevertheless, its mechanical properties and porosity persisted, remaining at the desirable levels. Its high toughness and low YM were consistent with the ductile nature of the formulation.

Table 3. Mechanical properties of samples after 3-month exposure in the Newberry well (standard deviations are given in parentheses)

Property	**Formulation**											
	1	2	3	4	5	6	7	8	9	10	11	12
Porosity (%)	34 (4)	44 (1)	36 (2)	38 (1)	45 (1)	48 (2)	37 (2)	44 (4)	39 (2)	35 (3)	42 (2)	40 (0.3)
Strength (psi)	4300 (645)	3600 (500)	4600 (700)	4000 (840)	3100 (20)	2500 (130)	4000 (170)	3100 (280)	3900 (125)	3600 (850)	2000 (300)	2300 (240)
YM (kpsi)	460 (32)	450 (30)	630 (18)	510 (37)	355 (20)	180 (10)	440 (30)	320 (37)	450 (15)	270 (70)	190 (60)	230 (3)
Tough. (Nmm/mm^3)	0.53 (0.12)	0.61 (0.04)	0.21 (0.03)	0.31 (0.09)	0.25 (0.06)	0.73 (0.15)	0.44 (0.08)	0.53 (0.12)	0.28 (0.07)	0.33 (0.02)	0.41 (0.06)	0.62 (0.15)

Figures 4 and 5 compare mechanical properties and water-fillable porosity of cement formulations after the initial 1-day autoclaving at 300°C and the 3-month exposure in Newberry well.

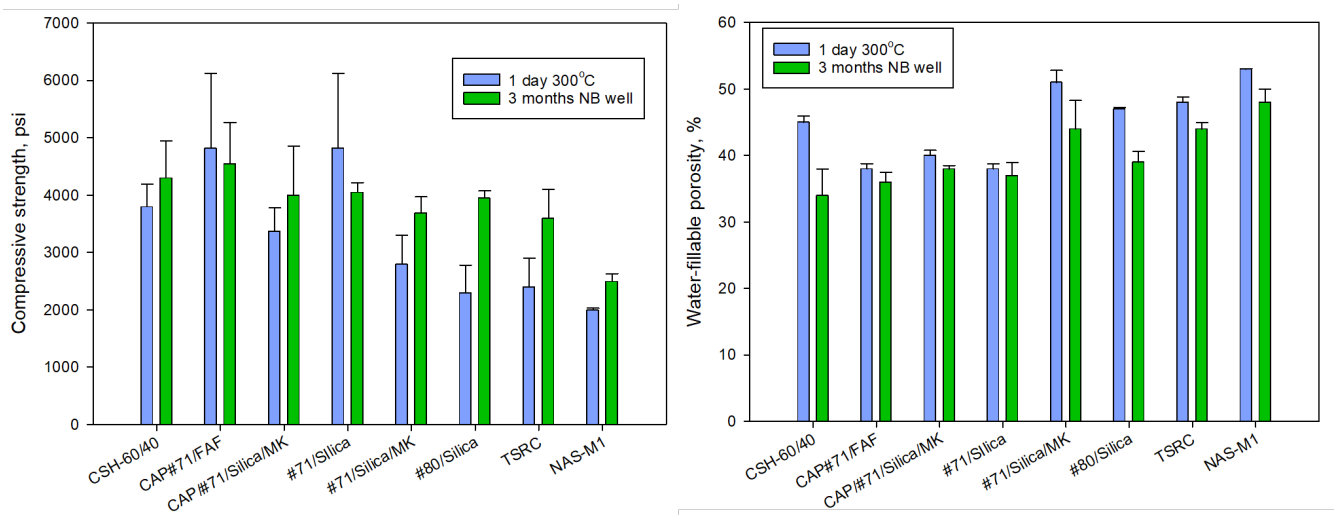

Figure 4: Compressive strength and water-fillable porosity of cement samples after 1-day 300°C autoclaving and the 3-month exposure in the Newberry well.

Without exception, the porosity of all the formulations decreased during the exposure tests. The strength increased for all formulations except #71/Silica one. However, it should be noted that

very high strength and the brittle nature of that cement after the original curing resulted in a large error bar.

The Young's modulus was indicative of brittle cements after the 3-month exposure for CAP cement formulations with CAC#71, for the- #71 cement with silica. Although the modulus of the reference OPC/silica formulation was among the top three, suggesting cement embrittlement during the exposure tests (Figure 5). Because of the embrittlement during the prolonged exposure cement toughness decreased dramatically for the CAP cement formulations with #71. Some toughness decrease was a general trend. However, for two cement formulations the toughness increased after the 3-month exposure – TSRC and gibbsite-based Ca-free cement.

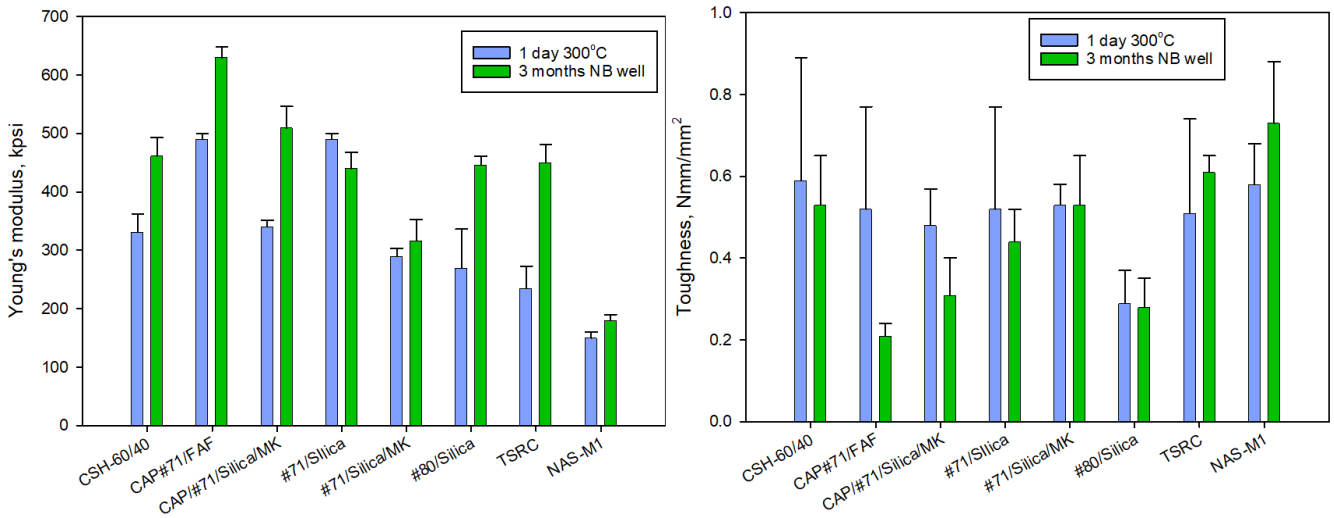

Figure 5: Young's modulus and toughness of cement samples after 1-day 300°C autoclaving and the 3-month exposure in the Newberry well.

Table 4 shows porosity and mechanical properties of the formulations exposed to the well conditions for 9 months.

After the 9-month exposure the only formulation that experienced dramatic deterioration of mechanical properties was the reference OPC/silica flour one. The original strength of 5170±390 psi dropped by 86% to 725±330 psi after the well exposure. Very low YM and toughness accompanied the strength decrease (62 kpsi and 0.19 N*mm/mm^3 respectively) (Table 4).

For all other formulations, rich in aluminum, the strength remained well above the requirement of 1000 psi.

As expected, chemical calcium phosphate cements had very high strength of around 5000 psi. Replacement of FAF with silica and MK resulted in lower strength (between 20 and 35% decrease depending on MK amount) but also lower YMs increasing cement ductility. This ductility improvement was reflected in higher toughness of the formulation with 10% MK.

CAC #71 and CAC #80 formulations with silica (#6 and #7 respectively) developed high strength (6515 psi and 4840 psi respectively) while their YM remained in the moderate range (329 and 304 kpsi respectively). This combination of high strength and relatively low YM was reflected in the very high toughness of these formulations (1.2 and 2 N*mm/mm^3, respectively).

Table 4. Mechanical properties of samples after 9-month exposure in the Newberry well (standard deviations are given in parentheses)

Property	Formulation											
	1	2	3	4	5	6	7	8	9	10	11	12
Porosity (%)	45 (5)	44 (0.8)	41 (1)	33 (1)	37 (1)	34 (1)	41 (1)	42 (1)	54 (1)	48 (1)	52 (1)	51 (1)
Strength (psi)	725 (330)	4770 (110)	5080 (1410)	7150 (550)	5640 (880)	6515 (1030)	4840 (850)	4750 (290)	2310 (230)	2360 (330)	1900 (400)	1450 (400)
YM (kpsi)	62 (27)	377 (30)	342 (97)	516 (123)	383 (34)	329 (91)	304 (49)	401 (11)	173 (56)	151 (28)	135 (80)	96 (38)
Tough. (Nmm/mm^3)	0.19 (0.12)	0.65 (0.27)	0.86 (0.16)	0.7 (0.08)	0.82 (0.14)	1.2 (0.51)	2 (0.34)	0.68 (0.06)	1.3 (0.9)	0.94 (0.48)	1.1 (0.46)	0.52 (0.14)

The compressive strength of the tested cements decreased in the order: CAP#71/FAF/MCF>#71/Silica/MCF>CAP#71/Silica/MK/MCF>CAP#50/FAF/MCF>#80/Silica /MCF>CAC#71/Silica/MK-2/MCF~TSRC/MCF>>NAS/CAC/Silica/MCF~NAS/CAC/Silica >NAS/MCF>NAS/Zr/MCF>> OPC/Silica/MCF.

The toughness as a combination of compressive strength and ductility followed a different order: #80/Silica/MCF>NAS/CAC/MCF>#71/Silica/MCF>NAS/MCF>NAS/CAC/Silica/MCF>CAP# 50/FAF/MCF>CAP#71/Silica/MK(10%)/MCF>CAP#71/FAF/MCF> CAP#71/Silica/MK(15%)/MCF~TSRC>NAS/Zr/MCF>>OPC/Silica/MCF.

The very strong cements are not necessarily the best choice for geothermal wells, especially EGS wells that undergo stimulation operations that can cause significant damage of brittle cement formulations.

Figures 6 and 7 compare mechanical properties and water-fillable porosity of cement formulations after the initial 1-day autoclaving at 300^{o}C and the 9-month exposure in Newberry well.

Apart from the reference OPC/Silica formulation that lost nearly all its original strength and a slight strength decrease of CAP#71/Silica/MK/MCF formulation, all the cement formulations increased their strength during the 9-month exposure tests. This increase was minor for CAP#71/FAF/MCF and gibbsite cement. It was significant for CAP#51/FAF/MCF, CAC#71 and #80 with silica (112%, 130%, and 124% respectively) and for TSRC (127%). The water-fillable porosity decreased for all cement formulations after the 9-month well exposure. Addition of MCF allows keeping moderate Young's modulus values despite significant increase of the strength for most cements. Only CAP#71/FAF/MCF formulation reached brittle failure modulus value above 500 kpsi. The Young's modulus below 400 kpsi for all other formulations persisted through the long-term well tests. These allowed several formulations, including CAC#71 or #80, gibbsite cement and CAP#50/FAF/MCF, achieving high toughness values nearly or above 1 N*mm/mm^3. The toughness of the formulation of #80/Silica reached 2 N*mm/mm^3. The reference formulations of OPC/Silica had very low values of both Young's modulus and toughness due to the cement degradation.

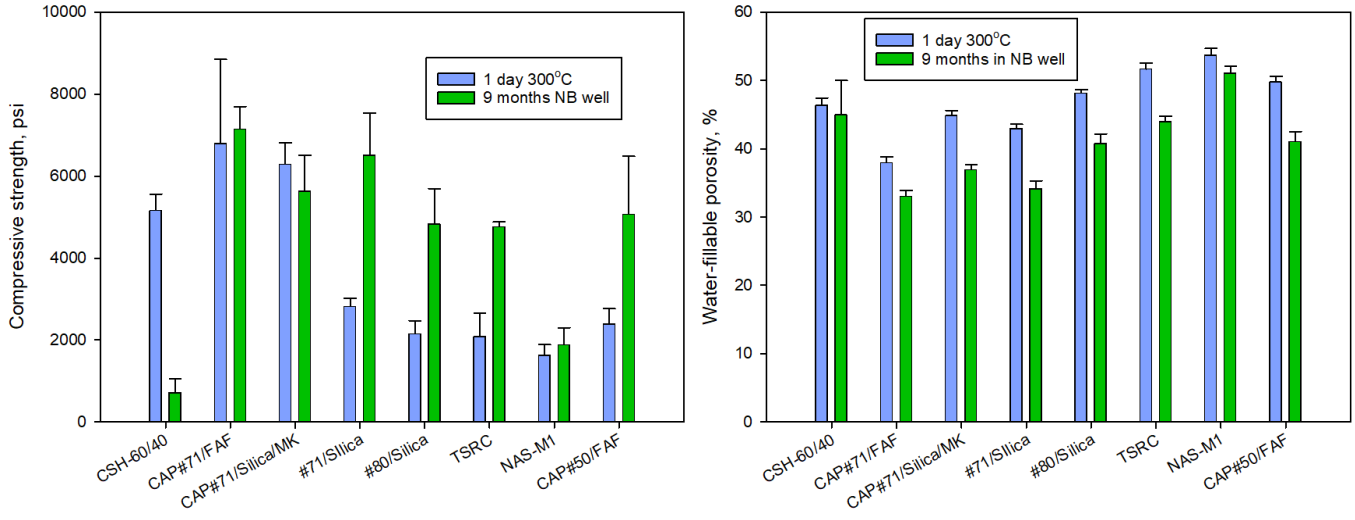

Figure 6: Compressive strength and water-fillable porosity of cement samples after 1-day 300ºC autoclaving and the 9-month exposure in the Newberry well. (Note: all the formulations contain MCF.)

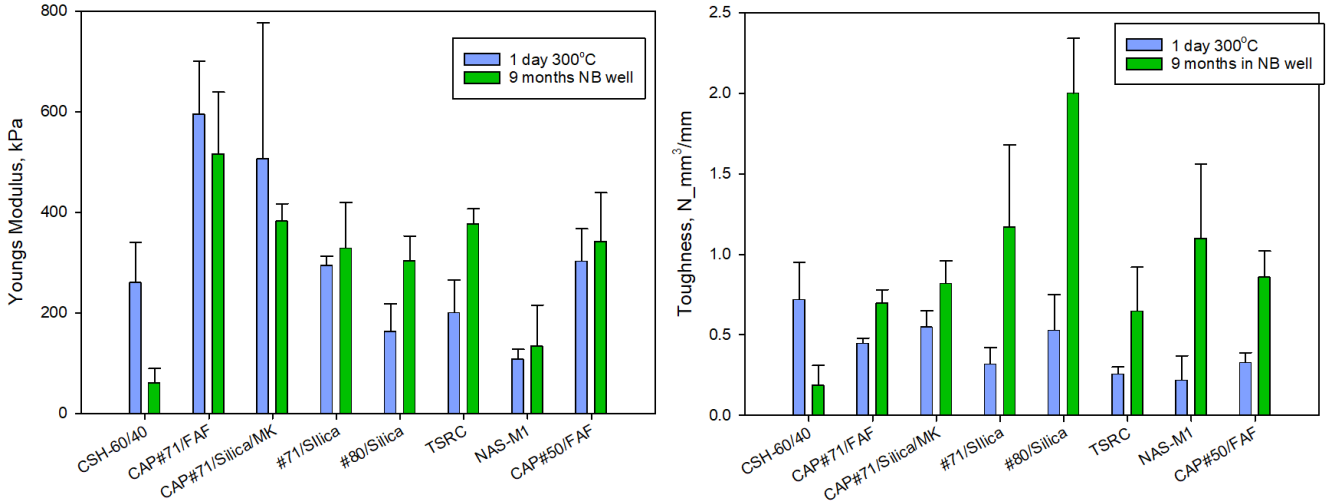

Figure 7: Young's modulus and toughness of cement samples after 1-day 300ºC autoclaving and the 9-month exposure in the Newberry well.

2.1.2.2. Phase compositions and Morphologies of selected formulations.

To understand changes in the mechanical properties of the exposed formulations and to predict their further stability and degradation under the well conditions, phase identification and morphological studies were performed for the designs of interest. Changes in the Portland cement-based formulation, CSH-60/40, that caused dramatic loss of mechanical properties without increasing the sample's porosity were of considerable interest.

2.1.2.2.1. CSH-60/40

Figure 8 shows the XRD patterns of the reference CSH-60/40 sample and those exposed in the well for 3 or 9 months.

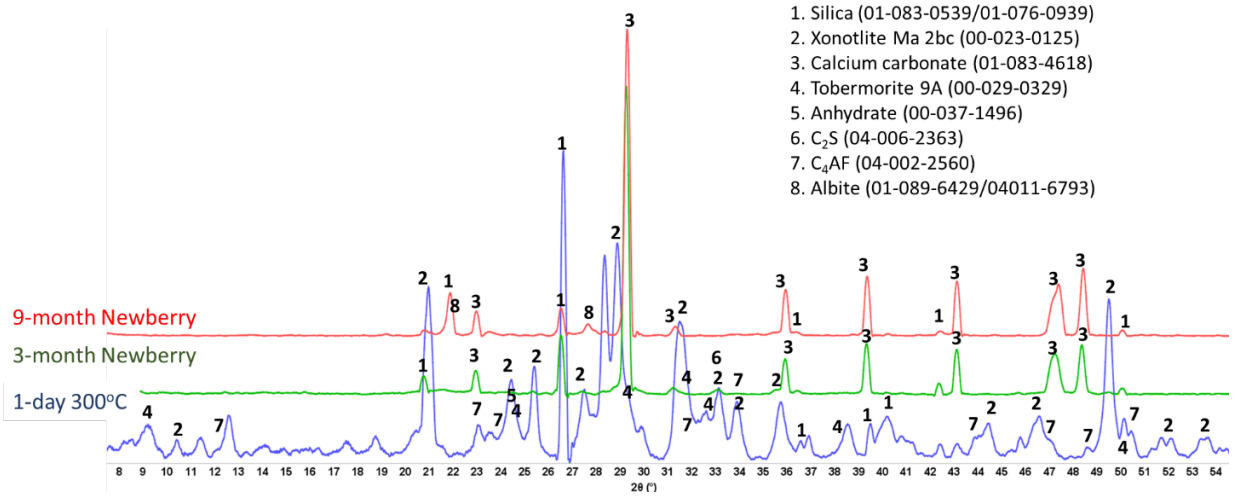

Figure 8. XRD patterns of the reference CSH-60/40 sample (after 1 day of autoclaving at 300 °C) and samples exposed in the Newberry well for 3 or 9 months.

For the CSH-60/40 formulation, the main crystalline phases of hydrated cement after one day of autoclaving at 300 °C were predictably tobermorite and xonotlite. Xonotlite should be the dominant crystalline phase at this temperature, with tobermorite temperature stability being below 200 °C (Taylor, 1997). Nevertheless, tobermorite was clearly present in the reference sample, although the intensity of xonotlite peaks was higher than for tobermorite ones. Further conversion of tobermorite to xonotlite after longer HT exposure was expected. This conversion is accompanied by microstructural changes with the growth of xonotlite needle crystals, resulting in slightly decreased strength and increased porosity. However, mechanical property analyses of this cement after the 3-month exposure revealed decreased sample porosity and increased strength. This unusual behavior can be understood from the results of the composition analyses.

For the field samples, xonotlite peaks were nearly absent from the XRD patterns. The patterns were dominated by the peaks of calcium carbonate and non-reacted silica. For the most part, the crystalline calcium–silicate phases converted to calcium carbonate. Only small xonotlite shoulders were still visible in the pattern of the 3-month exposed sample (e.g., 2 Θ ~28.8), but they completely disappeared from the patterns of the 9-month exposed samples. The only other crystalline phase detected by XRD was silica. The intensity of silica peaks decreased, suggesting that it, at least partially, participated in the tobermorite-to-xonotlite conversion before the sample was carbonated. The initial cement carbonation resulted in increased sample strength and decreased porosity due to the matrix densification with calcium carbonate.

However, after the longer 9-month exposure, calcium removal from calcium–silicate hydrates through carbonation resulted in a dramatic strength decrease. In the excess carbon dioxide and water vapors, calcium carbonate is converted into soluble calcium bicarbonate, which can migrate out of the cement matrix, leaving amorphous silica gel behind.

Strong sample carbonation was confirmed by the TGA/DTG tests (Figure 9). The only large decomposition event for both the 3- and 9-month exposed samples is carbonate's decomposition. The mass loss corresponding to this step is 21% and 28% after the 3- and 9-month exposures, respectively. A small decline in the weight curve associated with the cement hydrates was still

visible after 3 months in the well, while no weight loss associated with the cement hydrates was detected after the 9-month exposure. Assuming the decarbonation weight loss was only due to the calcium carbonate decomposition and knowing the initial weight percent of CaO in the class G cement (73%), the mass loss of 21% for the 60/40 cement/silica formulation means that 54% of the original calcium in the class G cement was in the form of carbonate after the 3 months of exposure. The 28% CO_2 loss during the decarbonation step of the OPC/silica formulation with 5% CMF corresponds to 83% of the calcium in the original formulation being carbonated. Considering that calcium carbonate was likely partially converted into the soluble calcium bicarbonate that could migrate from the samples, even higher conversion of the original calcium in the exposed samples is likely.

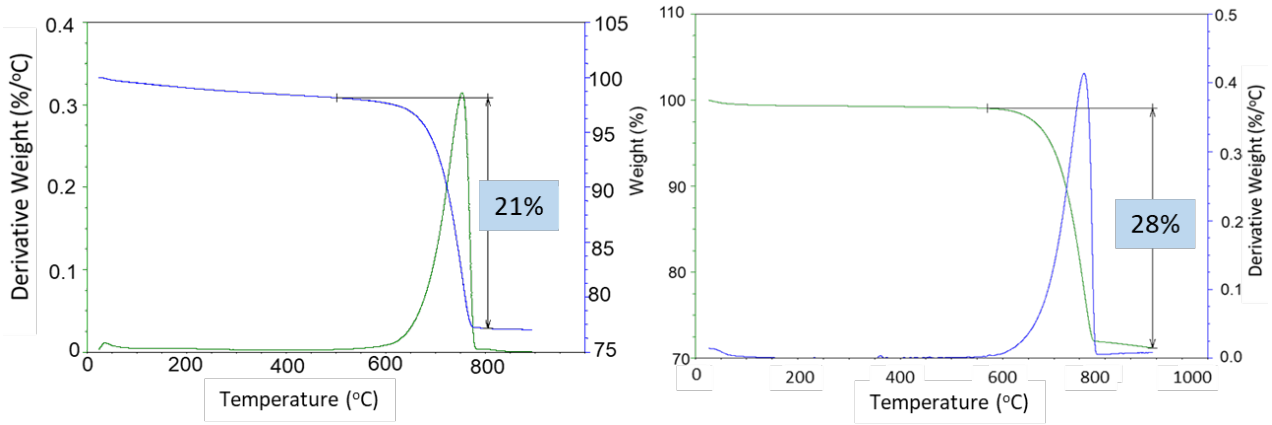

Figure 9. TGA/DTG curves of the CSH-60/40 samples exposed in the Newberry well for 3 months (left) or 9 months (right).

Figure 10 shows the morphologies of the 3- and 9-month exposed samples, and Table 5 provides the results of elemental composition measurements in representative locations.
The SEM images of the 3-month exposed sample show large calcium carbonate crystals (location 1) formed in an otherwise mostly amorphous cement matrix and smaller calcium carbonate crystals of different sizes (location 2) embedded into the matrix throughout the sample. In agreement with the XRD data, xonotlite needle-like crystals were not detected. Although well-formed, the large calcium carbonate crystals did not compromise the mechanical properties of the 3-month exposed samples. However, their precipitation did not prevent further sample carbonation, blocking CO_2 and water penetration into the sample. The large crystals in the images of the 9-month exposed samples belonged to non-reacted crystalline silica (location 4). Calcium carbonate crystals were not observed, the morphological features of the matrix became smaller, and the structure of the matrix had a porous aspect that would be favorable for continuous carbonation of the sample. The elemental composition in other tested locations corresponded to the calcium bicarbonate present along with silica gel (locations 3 and 5).

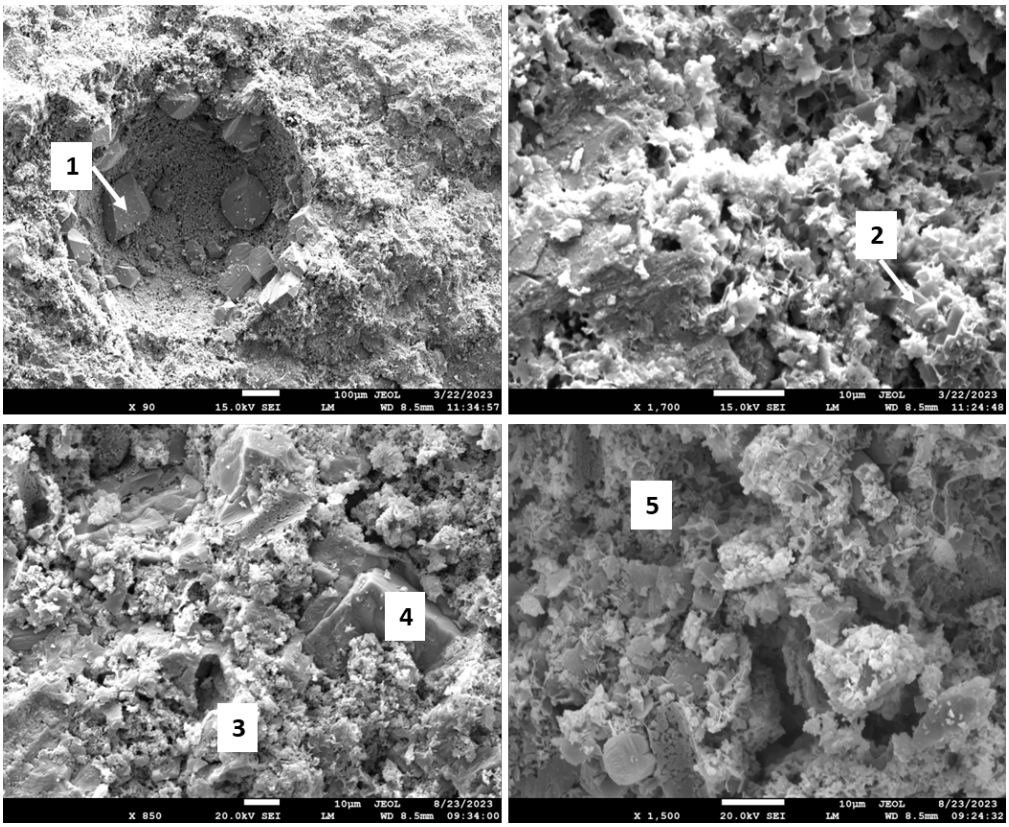

Figure 10. Photomicrographs of CSH-60/40 samples exposed in the Newberry well for 3 months (top) or 9 months (bottom).

Table 5. Elemental composition in the selected representative locations of the CSH-60/40 samples exposed in the Newberry well for 3 or 9 months (the locations of the analyses are shown in Figure 10).

Element	Location	Weight Percent (% Error)	Identified Phase	Location	Weight Percent (% Error)	Identified Phase
3-Month Exposure						
C	1	12.93 (0.45)	Calcium Carbonate ($CaCO_3$)	2	12.08 (0.52)	Calcium Carbonate ($CaCO_3$)
O		49.91 (1.20)			50.30 (0.90)	
Si		1.01 (0.10)			4.17 (0.14)	
Ca		35.07 (0.53)			31.11 (0.55)	
Fe		1.08 (0.29)			1.88 (0.31)	
9-Month Exposure						
C	3	9.65 (1.60)	Calcium bicarbonate ($CaHCO_3$)	4	8.93 (2.38)	Silica (SiO_2)
O		35.07 (0.91)			32.18 (1.03)	
Al		1.83 (0.14)			-	
Si		28.98 (0.63)			54.45 (1.52)	
Ca		19.28 (0.45)			2.63 (0.17)	
Fe		4.60 (0.30)			1.33 (0.27)	
C	5	11.94 (3.59)	Calcium bicarbonate ($CaHCO_3$)			
O		26.00 (2.00)				
Al		2.44 (0.38)				
Si		24.43 (1.32)				
Ca		16.69 (0.99)				
Fe		18.50 (1.34)				

In summary, for the CSH-60/40 formulation, the results of all the analyses agreed. This formulation underwent severe carbonation in the well, resulting in its loss of mechanical properties. Its water-fillable porosity nevertheless persisted, with calcium carbonates forming a matrix with relatively low permeability.

2.1.2.2.2. Calcium Phosphate Cement with Different CAC Grades (CAP#71/FAF, CAP#50/FAF)

Calcium phosphate cement formulations were specifically developed to withstand CO_2-reach HT environments in geothermal wells (Sugama et al., 1995; Weber et al., 1998). The CO_2-resistance of this cement comes from CO_2 mineralization with the formation of stable carbonated apatite and cancrinite phases [49]. The two formulations of CAP cement with FAF were made with CAC#71 and with CAC#50. CAC#71 has a higher aluminum content (55.8 wt.% Al_2O_3) and a lower Ca content (44.0 wt.% CaO) than CAC#50 (45.1% and 49.7%, respectively). Figures 11 and 12 show XRD patterns of these formulations for the reference samples and samples exposed in the well for 3 or 9 months.

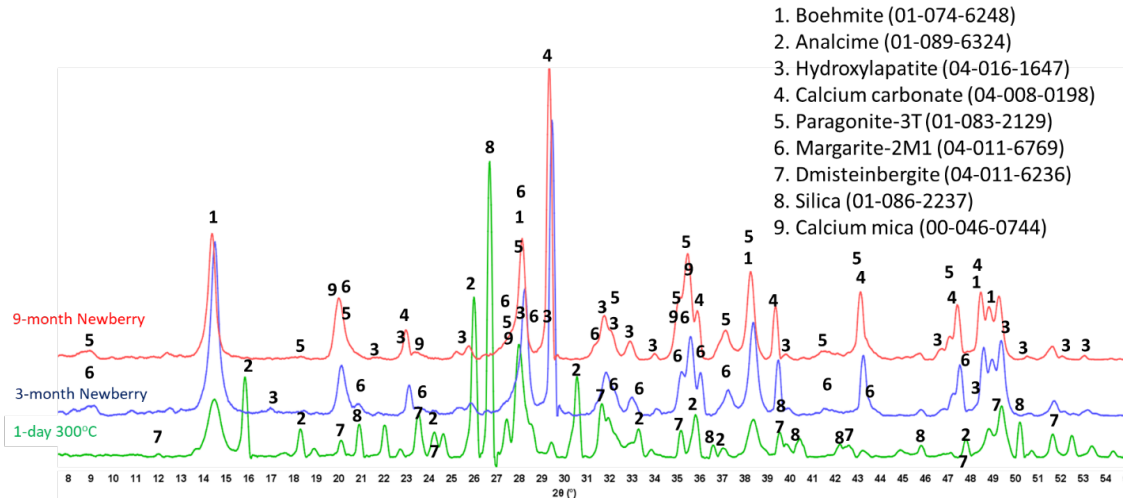

Figure 11. XRD patterns of the reference CAP#71/FAF sample (after 1 day of autoclaving at 300 °C) and samples exposed in the Newberry well for 3 or 9 months.

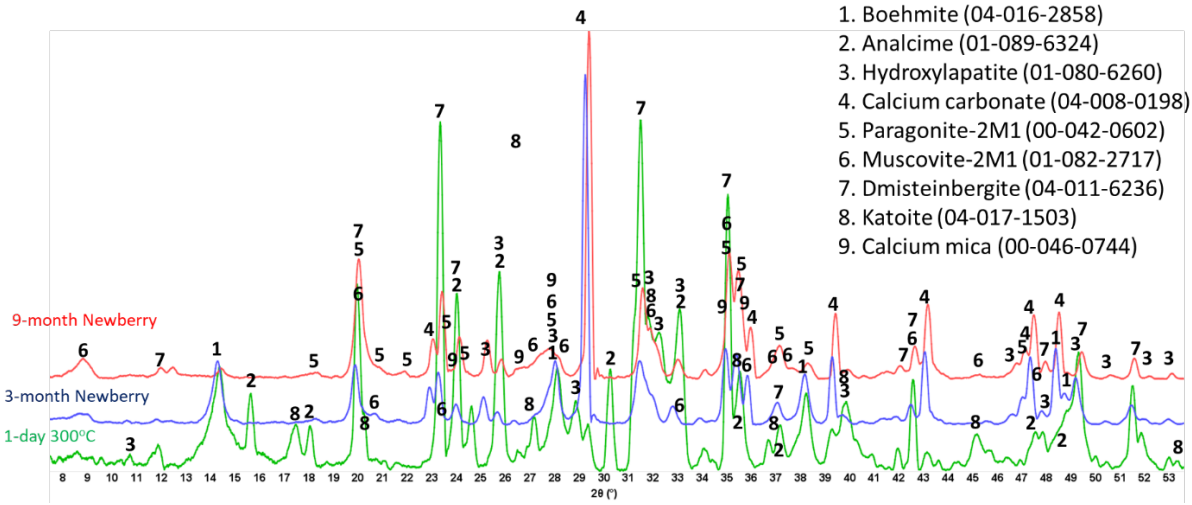

Figure 12. XRD patterns of the reference CAP#50/FAF sample (after 1 day of autoclaving at 300 °C) and samples exposed in the Newberry well for 3 or 9 months.

The reference patterns include expected phases of boehmite (aluminum oxide hydroxide), hydroxylapatite and analcime, high-temperature stable zeolite, and the feldspar mineral dmisteinbergite ($CaAl_2Si_2O_8$), an isomorph of anorthite. In the formulation with CAC#50, which is richer in calcium, crystallization of katoite takes place ($Ca_3Al_{3.5}O_{4.5}(OH)_{7.5}$). This phase is absent in CAP#71/FAF with more aluminum-rich CAC#71.

Samples exposed to the well resulted in the disappearance of analcime peaks in both formulations and the disappearance of katoite peaks in CAP#50/FAF. The intensity of boehmite peaks strongly dropped in CAP#50/FAF with lower aluminum content but remained strong in CAP#71/FAF. The intensity of the dmisteinbergite peaks decreased in both formulations. The new peaks of mica-type minerals appeared in the patterns. These were identified as belonging to paragonite, margarite, muscovite, and Ca-mica minerals. Calcium carbonate peaks were present in the patterns of both formulations.

The peaks of hydroxylapatite were clearly present in the patterns of both formulations. However, the expected carbonated phases of cancrinite and carbonated apatite were not found. If for carbonated apatite, phase identification is somewhat problematic due to the strong patterns overlapping with the apatite phase peaks and the low crystallinity of the newly formed carbonated apatite phase during CAP cement carbonation, the phase of cancrinite could be identified if it formed in the samples.

Partial carbonation of the samples was confirmed with TGA/DTG and EDX analyses (Figure 13). The two major weight loss events in thermogravimetric experiments of CAP cement formulations were the decomposition of boehmite between 400 and 550 °C and the decarbonation of the samples above 600 °C (Foldvari, 2011). The weight loss associated with boehmite dehydroxylation was 5% and 4% after 3 and 9 months of well exposure for CAP#71/FAF and 3 and 1.5% for CAP#50/FAF, respectively (Figure 14). This result agreed with the strongly decreased peak intensities of boehmite in 9-month exposed CAP#50/FAF samples. The extent of carbonation for CAP#71/FAF formulation did not change between 3 and 9-month exposures, persisting at 8%.

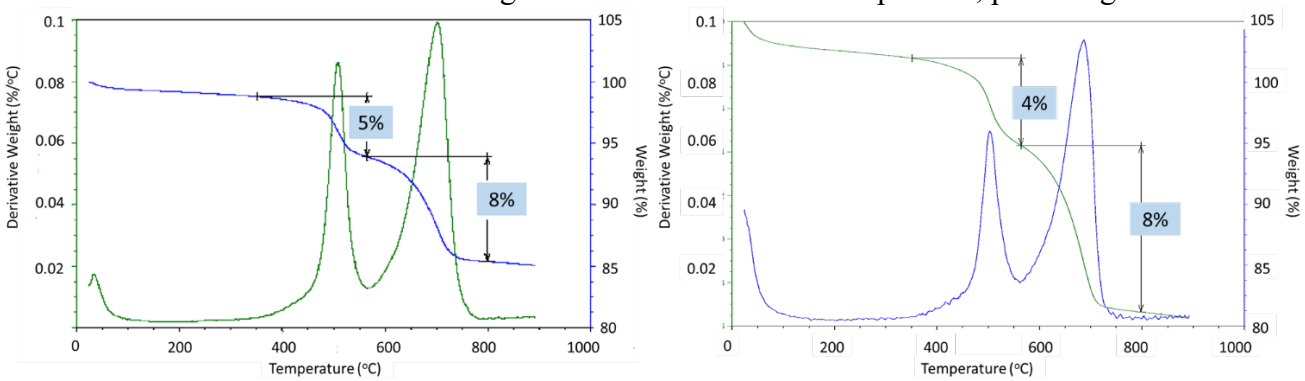

Figure 13. TGA/DTG curves of the CAP#71/FAF samples exposed in the Newberry well for 3 months (left) or 9 months (right).

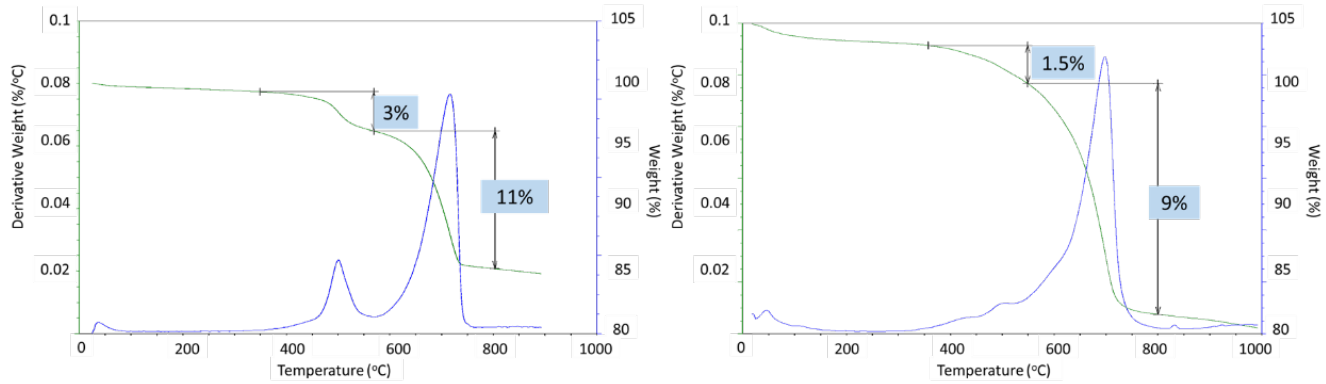

Figure 14. TGA/DTG curves of the CAP#50/FAF samples exposed in the Newberry well for 3 months (left) or 9 months (right).

For CAP#50/FAF, the decarbonation peak was slightly smaller after 9 months in the well (9% vs. 11% after the 3-month exposure). The decrease in carbonate concentration during longer exposures could be attributed to the continued carbonation and removal of soluble carbonates from the sample. However, it is likely that samples did not undergo any significant additional carbonation, as in the case of the CSH-60/40 formulation, since the percent of decarbonation did not increase.

The results of morphological analyses are shown in Figures 15 and 16, and the EDX compositions along with the phases identified in selected locations are shown in Tables 6 and 7.

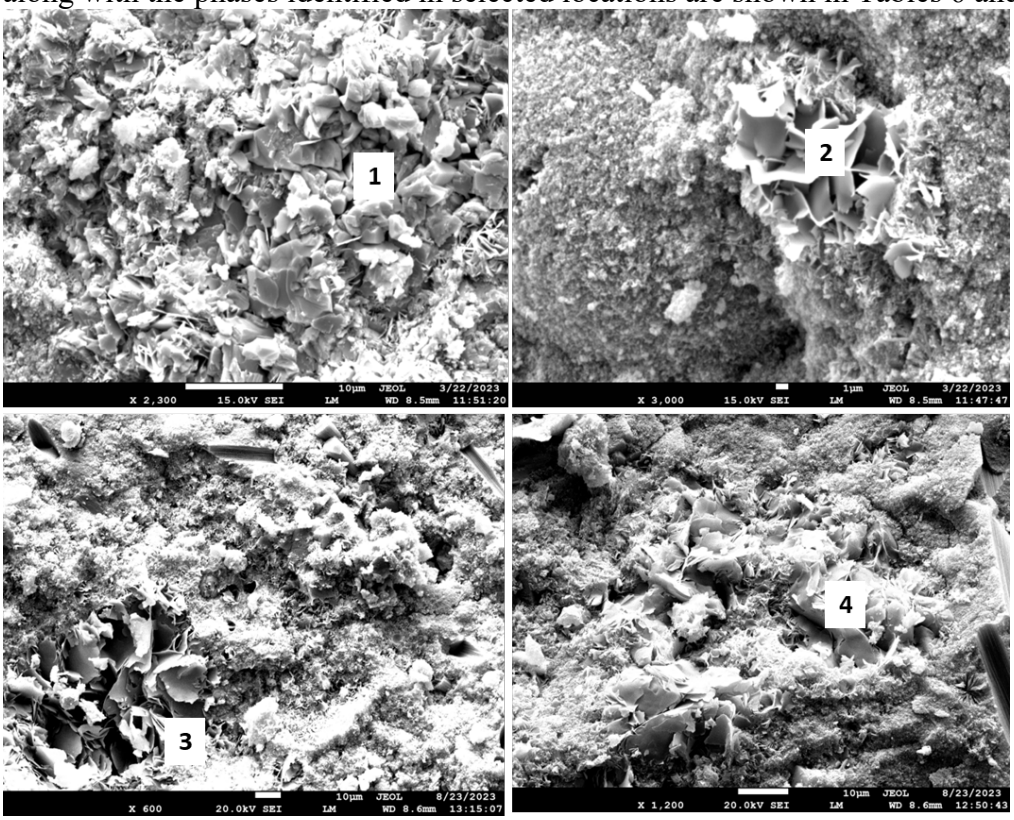

Figure 15. Photomicrographs of CAP#71/FAF samples exposed in the Newberry well for 3 months (top) or 9 months (bottom).

Table 6. Elemental composition in the selected representative locations of the CAP#71/FAF samples exposed in the Newberry well for 3 or 9 months (the locations of the analyses are shown in Figure 15).

Element	Location	Weight Percent (% Error)	Identified Phase	Location	Weight Percent (% Error)	Identified Phase
3-Month Exposure						
C	1	11.7 (0.45)	Calcium Carbonate ($CaCO_3$)	2	-	Dmisteinbergite ($CaAl_2Si_2O_8$)
O		48.30 (1.2)			43.02 (0.90)	
Si		-			16.66 (0.40)	
Ca		38.01 (0.57)			9.24 (0.43)	
Al		1.26 (0.11)			18.99 (0.40)	
Fe		-			12.09 (0.93)	
9-Month Exposure						
O	3	30.05 (0.66)	Calcium mica ($Al_3Ca_{0.5}Si_3O_{11}$) or Margarite ($(Na_{0.2}Ca_{0.8}Al_{3.9}Si_{2.1})_{11}(OH)$)	4	36.14 (0.53)	Margarite ($(Na_{0.2}Ca_{0.8}Al_{3.9}Si_{2.1})_{11}(OH)$)
Na		1.22 (0.20)			2.01 (0.18)	
Al		27.85 (0.38)			27.26 (0.31)	
Si		26.16 (0.40)			25.69 (0.33)	
K		4.52 (0.20)			2.82 (0.15)	
Ca		7.64 (0.24)			4.69 (0.17)	
Fe		2.11 (0.35)			1.39 (0.23)	

Table 7. Elemental composition in the selected representative locations of the CAP#50/FAF samples exposed in the Newberry well for 3 or 9 months (the locations of the analyses are shown in Figure 16).

Element	Location	Weight Percent (% Error)	Identified Phase	Location	Weight Percent (% Error)	Identified Phase
3-Month Exposure						
C	1	10.91 (0.65)	Multiple, amorphous matrix	2	-	Hydroxylapatite, aluminum-silicate matrix
O		56.90 (0.90)			45.68 (0.80)	
Na		0.89 (0.10)			0.77 (0.16)	
Al		14.81 (0.32)			23.53 (0.24)	
Si		9.57 (0.23)			12.12 (0.21)	
P		0.93 (0.09)			4.13 (0.17)	
Ca		4.75 (0.16)			12.39 (0.24)	
Fe		1.24 (0.20)			1.38 (0.32)	
9-Month Exposure						
O	3	38.34 (0.74)	Calcium–aluminum–silicate matrix	4	30.05 (0.59)	Margarite ($(Na_{0.2}Ca_{0.8}Al_{3.9}Si_{2.1})_{11}(OH)$)
Na		1.31 (0.22)			1.19 (0.20)	
Al		19.26 (0.32)			23.89 (0.32)	
Si		19.28 (0.35)			23.46 (0.34)	
K		2.64 (0.15)			2.78 (0.15)	
Ca		15.92 (0.30)			4.15 (0.16)	

In agreement with the XRD and TGA/DTG data, the CAP#71/FAF formulation had some inclusions of calcium carbonate crystals after the 3-month exposure (location 1). The matrix also still contained non-reacted FAF particles (top right photomicrograph, Figure 15) and clearly identifiable dmisteinbergite crystals (location 2). After the 9-month exposure, the larger crystalline features similar to dmisteinbergite and more compact embedded into the dense matrix had compositions related to mica-type minerals, margarite, with its typical morphology of a mass with thin laminae, and Ca-mica (locations 3 and 4).

The photomicrographs of CAP#50/FAF samples are presented in Figure 16, and Table 7 shows EDX elemental analyses at specified locations and possible corresponding phases. The 3-month

well-exposed sample matrix was very dense and rich in aluminum and silica, with the presence of phosphorus, calcium, and some iron (location 1). Carbon detection indicated partial matrix carbonation; however, large calcium carbonate crystals were not found in the sample. Non-reacted particles of FAF were still visible (photograph, top right) embedded into the matrix. EDX analyses showed that phosphorus phases made up part of small crystals of less than 1 micron or were incorporated into the amorphous matrix. After the 9-month exposure, a dense matrix was formed with tiny crystals of calcium mica (locations 2, 3 and 4). The photomicrograph also shows intact carbon fibers that withstood a 9-month exposure in the bulk cement without any visible damage.

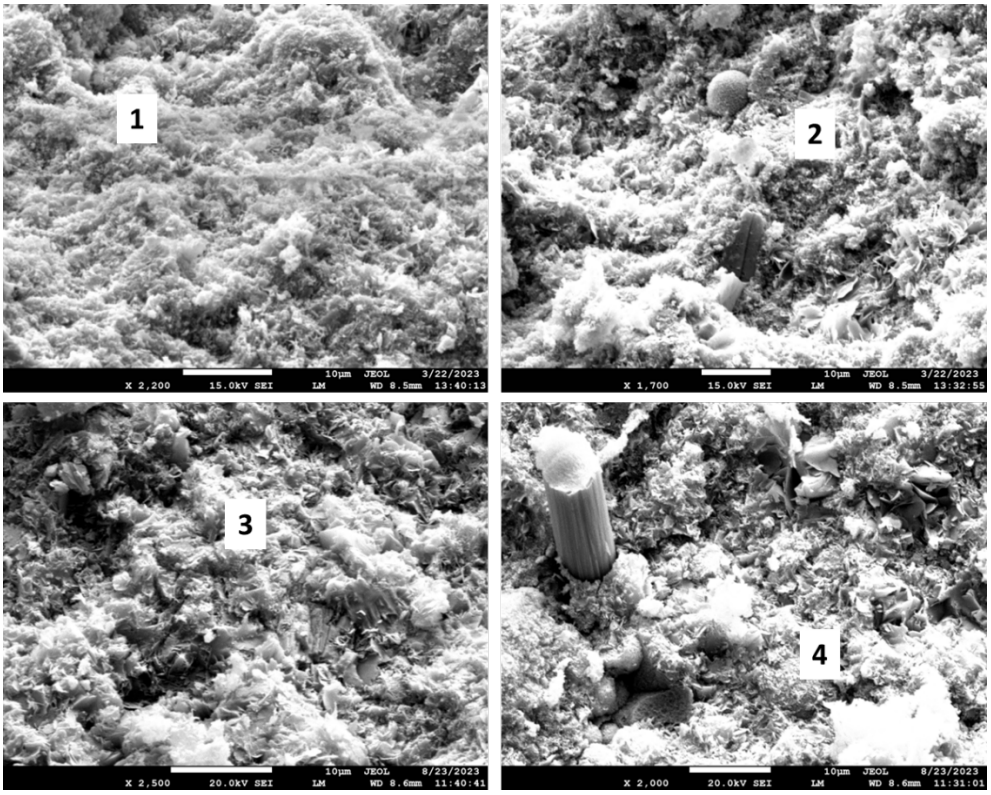

Figure 16. Photomicrographs of CAP#50/FAF samples exposed in the Newberry well for 3 months (top) or 9 months (bottom).

In summary, CAP cement formulations underwent only partial carbonation during the well exposure tests. The crystalline composition of these samples persisted through the exposure, with the major crystalline phases of dmisteinbergite, paragonite, and hydroxylapatite remaining in the samples after the 9-month exposure. The extent of the carbonation was higher for the more Ca-rich CAP#50/FAF formulation than for the CAP#71/FAF one with a lower calcium content. Persistent crystalline compositions and a dense matrix with limited carbonation provided improved mechanical properties and a very low water-fillable porosity for these formulations.

2.1.2.2.3. TSRC

Like CAP cement, TSRC was developed to withstand high thermal shocks typical for HT geothermal wells and was also expected to mineralize CO_2 into a stable cancrinite phase (Pyatina & Sugama, 2018). This blend is based on CAC#80 with the lowest calcium (24.7 wt.%) and highest

aluminum (75.2 wt.%) contents. This Al-rich composition, combined with the FAF, provides high thermal shock resistance for the blend.

Figure 17 presents the XRD patterns of the TSRC reference samples and samples exposed in the well for 3 or 9 months. The reference sample crystalline composition was very similar to that of CAP/FAF formulations, except for the phosphorus-containing phases that were absent in TSRC and the presence of corundum (aluminum oxide) crystals from CAC#80 in the TSRC formulation. The major crystalline phases include dmisteinbergite and its isomorph anorthite, analcime, katoite, boehmite, and non-reacted mullite from FAF. After the 3-month well exposure, analcime, katoite, and mullite peaks disappeared, while new peaks of paragonite, margarite, and calcium carbonate showed up in the pattern, and peaks of boehmite persisted. After the 9-month exposure, boehmite peaks vanished from the sample pattern, while the peaks of paragonite, margarite, and calcium carbonate persisted. Although the patterns of dmisteinbergite overlap with other phases identified in the exposed samples, its peaks at 2θ of 24.08 and 31.5 were clearly identifiable in the exposed samples. The persistence of crystalline phases implies their stability over the exposure time under the well conditions, which is further supported by the similarity of the patterns of the 3- and 9-month exposed samples.

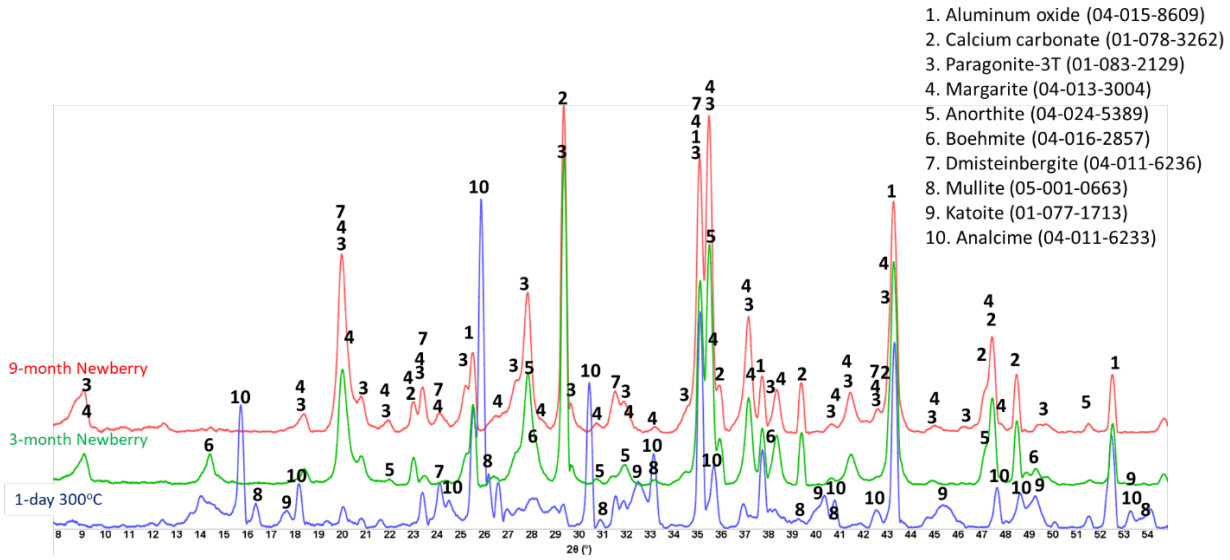

Figure 17. XRD patterns of the reference TSRC sample (after 1 day of autoclaving at 300 °C) and samples exposed in the Newberry well for 3 or 9 months.

The TGA/DTG analyses confirmed partial carbonation of the sample (Figure 18). In agreement with the XRD data, the two main weight loss events were from the dehydroxylation of boehmite (1% weight loss in the 3-month exposed sample and 0.4% weight loss in the 9-month exposed sample) and decarbonation of the samples (8 and 7%, respectively). This data confirmed the disappearance of boehmite after longer well exposure and the persistence of carbonation, which, unlike for the CSH-60/40 formulation, did not increase after longer exposure. The slight decrease in decarbonation weight loss could be attributed to the partial dissolution of the carbonates.

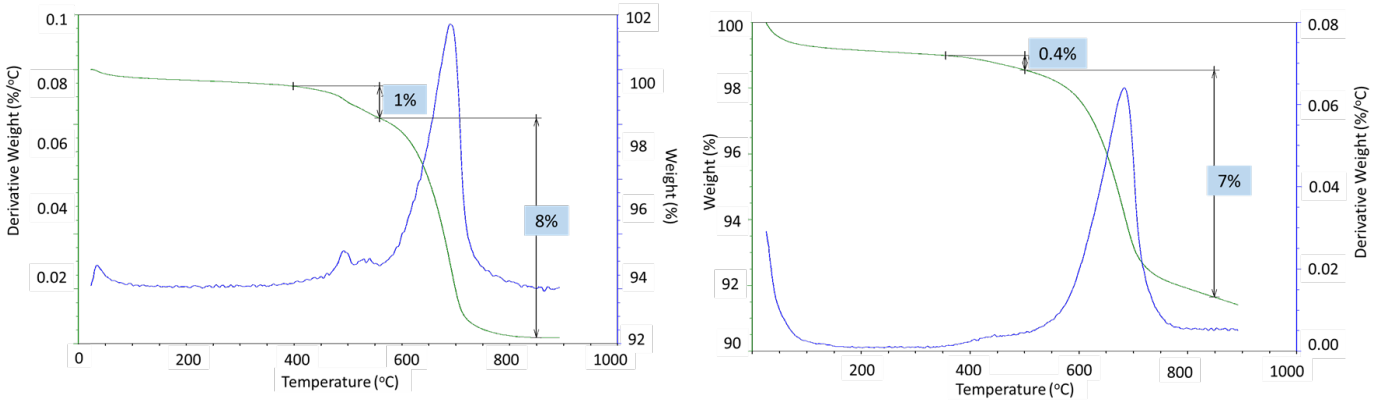

Figure 18. TGA/DTG curves of the TSRC samples exposed in the Newberry well for 3 months (left) or 9 months (right).

Figure 19 shows the microstructures of the exposed samples, and Table 8 provides their elemental compositions in selected locations along with the suggested phases. The morphological study of the 3-month exposed samples showed non-reacted FAF particles (top left photomicrograph) remaining in the samples. Pozzolanic reactions of these particles provide self-healing properties of the cement, so their presence in the cement matrix suggests that cement still possessed self-healing properties after the 3-month exposure. In agreement with the XRD data, these samples contained boehmite plates (location 1) and margarite crystals embedded into the dense matrix (location 2). The 9-month exposed samples showed feldspar minerals anorthite (location 3) and dmisteinbergite (location 4). The cubic crystal surrounded by dmisteinbergite plates is calcium carbonate. The possible pathway for such close co-existence of these crystalline structures is the transformation of dmisteinbergite into calcium carbonate during the longer exposure. As in the CAP#50/FAF samples, there was no visible damage to carbon fibers from the exposure of TSRC, despite their 2–3 orders of magnitude higher pore water pH than that of CAP#50/FAF.

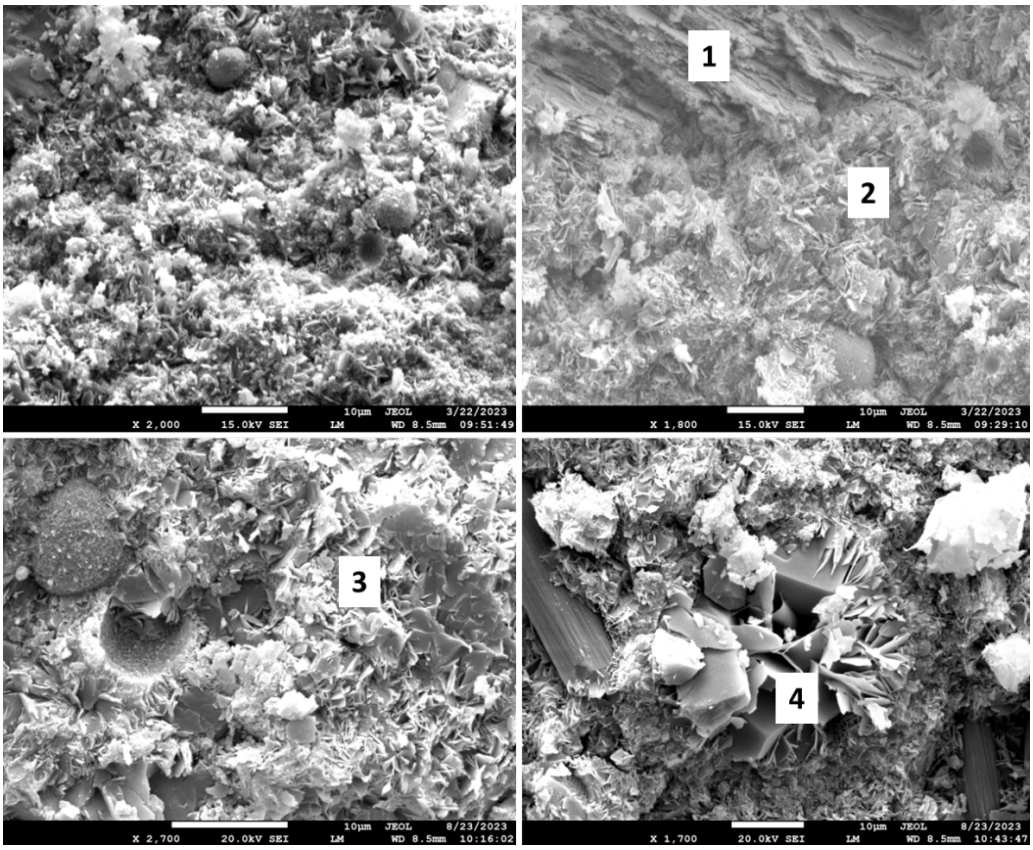

Figure 19. Photomicrographs of TSRC samples exposed in the Newberry well for 3 months (top) or 9 months (bottom).

Table 8. Elemental composition in the selected representative locations of the TSRC samples exposed in the Newberry well for 3 or 9 months (the locations of the analyses are shown in Figure 19).

Element	Location	Weight Percent (% Error)	Identified Phase	Location	Weight Percent (% Error)	Identified Phase
3-Month Exposure						
O	1	47.68 (0.52)	Boehmite (AlOOH)	2	48.08 (0.85)	Margarite ($CaAl_4Si_2O_{10}(OH)_2$)
Al		47.73 (0.41)			31.71 (0.28)	
Si		4.59 (0.31)			15.95 (0.24)	
Ca		-			4.26 (0.21)	
9-Month Exposure						
O	3	28.64 (0.75)	Anorthite, potassium bearing (like (Ca, Na) ($Si,Al)_4O_8$)	4	38.99 (0.62)	Dmisteinbergite ($CaAl_2Si_2O_8$)
Na		-			1.61 (0.18)	
Al		25.62 (0.39)			19.23 (0.28)	
Si		30.11 (0.46)			14.56 (0.27)	
K		6.96 (0.25)			1.37 (0.13)	
Ca		6.81 (0.26)			23.16 (0.33)	
Fe		1.86 (0.39)			1.08 (0.26)	

In summary, the TSRC formulation, designed to withstand the HT thermal shocks of geothermal wells, was also stable under the conditions of the Newberry well. Its crystalline composition persisted, and carbonation was limited, which resulted in improved mechanical properties and decreased water-fillable porosity. Moreover, the persistence of FAF in the composition of the blend suggests that it kept its self-healing properties for months at very high temperatures.

2.1.2.2.4. #80/Silica

This simple two-component blend showed significant improvement in its mechanical properties (especially toughness) and decreased water-fillable porosity during the exposure tests. Refractive CAC#80 is well-suited for the HT geothermal conditions (Sugama & Pyatina, 2018). The XRD patterns of the reference sample (1 day at 300 °C) and samples exposed to 3- and 9-month well conditions are shown in Figure 20.

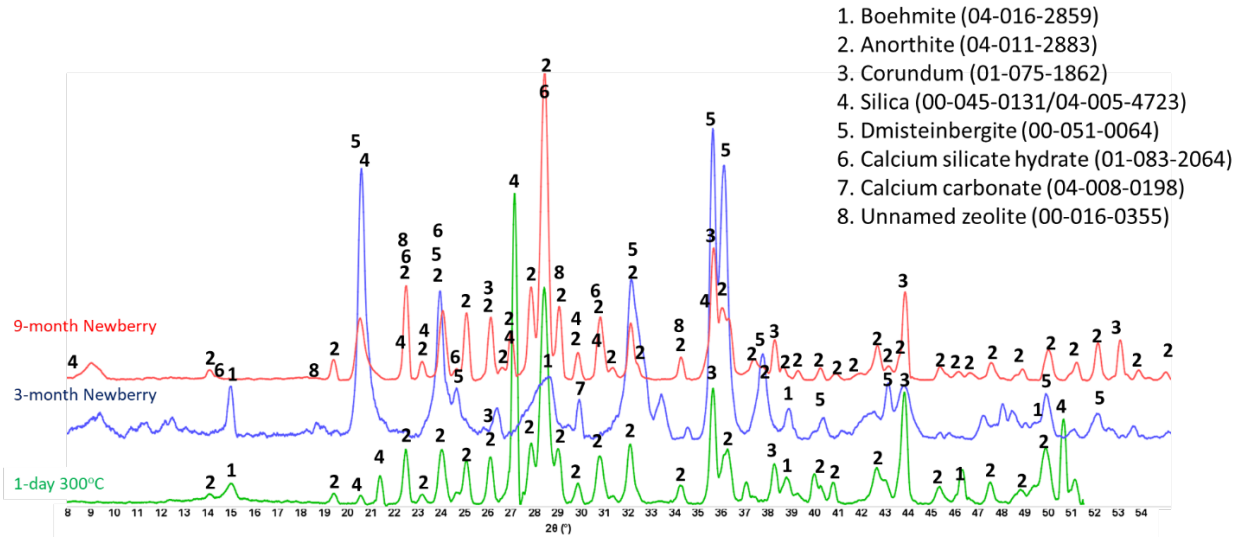

Figure 20. XRD patterns of the reference #80/Silica sample (after 1 day of autoclaving at 300 °C) and samples exposed in the Newberry well for 3 or 9 months.

The pattern of the reference sample included CAC#80 hydration product boehmite, CAC#80 and silica reaction product anorthite, and non-reacted phases corundum from CAC#80 and silica. Exposure of the sample to the Newberry well conditions resulted in the formation of anorthite isomorph dmisteinbergite after the 3-month exposure and calcium silicate hydrate ($Ca_{6.43}(Si_2O_7)_2(H_2O)_2$), as well as unnamed zeolite ($K_{2.84}Ca_{1.43}Al_{5.7}Si_{10.3}O_{32}*10.6H_2O$) after the 9-month exposure. Since the intensity of anorthite peaks was similar after 3 and 9 months, while that of dmisteinbergite decreased after the 9-month exposure, it is reasonable to think that the dmisteinbergite isomorph underwent partial conversion into albite while anorthite persisted. In the unnamed zeolite cation, calcium is replaced by potassium. The original formulations did not contain any alkaline activators, which means that potassium ions came from the well fluids. A small peak of calcium carbonate appeared in the field exposed samples. The TGA/DTG tests showed that decarbonation accounted for less than 2% of mass loss after 3 months of the well exposure and less than 1.5% mass loss after 9 months of the exposure (Pyatina & Sugama, 2023).

The morphological study of the samples confirmed the XRD results (Figure 21, Table 9). Dmisteinbergite (location 1) and boehmite (location 2) were detected in the 3-month exposed sample. Partial degradation of the boehmite crystals with the formation of a fluffy amorphous phase around them is visible in the photomicrograph (location 2). The 9-month exposed samples showed sites with typical anorthite morphology and elemental composition (location 3) and the elemental composition of the unnamed zeolite around the crystals with dmisteinbergite morphology (location 4). Boehmite crystals were not detected in the 9-month exposed samples, in agreement with the XRD results. The morphological features of these samples were small. As for other formulations, intact carbon fibers were visible in the 9-month exposed sample.

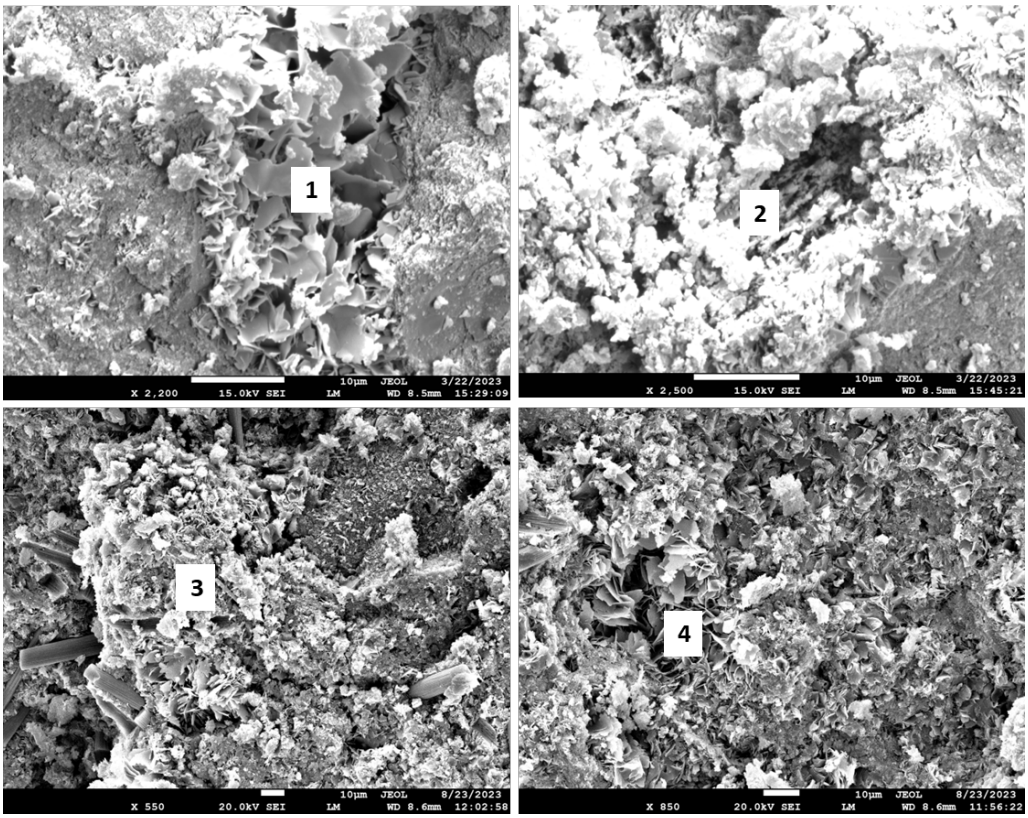

Figure 21. Photomicrographs of #80/Silica samples exposed in the Newberry well for 3 months (top) or 9 months (bottom).

Table 9. Elemental composition in the selected representative locations of the #80/Silica samples exposed in the Newberry well for 3 or 9 months (the locations of the analyses are shown in Figure 21).

Element	Location	Weight Percent (% Error)	Identified Phase	Location	Weight Percent (% Error)	Identified Phase
3-Month Exposure						
O	1	46.84 (0.9)	Dmisteinbergite ($CaAl_2Si_2O_8$)	2	43.98 (0.05)	Boehmite (AlOOH)
Al		22.02 (0.52)			40.21 (0.35)	
Si		20.03 (0.59)			2.63 (0.25)	
Ca		11.11 (0.59)			10.34 (0.29)	
9-Month Exposure						
O	3	29.48 (1.02)	Anorthite, potassium bearing (like (Ca, Na) (Si, $Al)_4O_8$)	4	31.11 (1.17)	Unnamed zeolite ($K_{2.84}Ca_{1.43}Al_{5.7}Si_{10.3}O_{32}$ $10.6H_2O$)
Na		1.17 (0.29)			1.33 (0.33)	
Al		23.82 (0.49)			21.30 (0.54)	
Si		25.54 (0.56)			23.68 (0.62)	
K		4.30 (0.31)			10.48 (0.45)	
Ca		15.68 (0.46)			12.10 (0.52)	

In summary, the #80/Silica formulation showed good resistance to the conditions of the HT geothermal well. The feldspar minerals formed during the blend hydration were partially converted into the alkali plagioclase series member albite and an unnamed zeolite, with the alkaline ions coming from the well environment. The carbonation of the blend was minimal.

2.1.3. Discussion

Exposure of various cementitious blends in a deep HT geothermal well for up to 9 months allowed evaluation of their performance under field conditions that would be very difficult to reproduce in laboratory tests. Although the samples were originally cured hydrothermally in laboratory environments (1 day at 300 °C), the general tendencies in the behavior of different blends can be deduced from the results of the exposure tests. Among the tested formulations, only CSH-60/40 was a calcium–silicate blend of OPC and silica. The rest included CAC, and NAS-M1 was calcium-free. The well environment was rich in CO2, with a well temperature and pressure (300–350 °C and 26 MPa, respectively) indicative of its supercritical state. It is likely that other geological fluids/gases were also present in the well.

Even though all tested blends underwent phase transitions under the well conditions over the long exposure times, all of them except the CSH-60/40 maintained, and often improved, their mechanical properties and decreased water-fillable porosity after the 9-month exposure. Although persisting, the mechanical properties of the NAS-M1 sample remained lower than for other Al-rich formulations, while the porosity was higher. Optimization of this formulation will require further efforts.

The dramatic loss of CHS-60/40's mechanical properties (86% strength loss) after the 9-month exposure coincided with the blend's severe carbonation (83% of the original calcium was carbonated based on the results of TGFA analyses). If the initial blend carbonation with precipitation of calcium carbonate in the pores after the 3-month exposure resulted in improved strength (13% increase) and decreased porosity (24% decrease), further carbonation compromised the samples' performance through the formation of soluble calcium bicarbonate and amorphous silica gel according to the following reactions:

$CO_2 + H_2O = H^+ + HCO_3^-$

C-S-H phase + $H^+ + HCO_3^- = CaCO_3$ + amorphous gel

$CaCO_3 + CO_2 + H_2O = Ca(HCO_3)_2$

OPC/silica decomposition due to carbonation in less than 9 months significantly disagrees with multiple other works cited in the introduction on Portland cement carbonation rates. This is likely due to the severity of the well environment, where HT supercritical CO2 reactions with the cement were dramatically accelerated. It should also be mentioned that the samples were relatively small in volume (12.6 cm3), facilitating their carbonation. Nevertheless, the long-term stability of OPC-based cements under such conditions could hardly be expected, even for larger cement volumes.

Formulations based on CAC all experienced partial carbonation through the calcium reaction, resulting in the formation of calcium carbonate. These formulations did not form any calcium–silicate hydrates after the initial 1-day curing at 300 °C. They all formed the plagioclase minerals anorthite and dmisteinbergite. The HT carbonation of anorthite/dmisteinbergite can be summarized in the following reaction (Fischer et al., 2011; Oelkers et al., 2008):

$CaAl_2Si_2O_8 + CO_2 + 2H_2O = CaCO_3 + Al_2Si_2O_5(OH)$

The reaction proceeds in solution after the dissolution of carbon dioxide and anorthite [53].

$CO_2 + H_2O = H^+ + HCO_3^-$

$CaAl_2Si_2O_8 + 16H^+ = Ca_{aq}^{2+} + 2Al_{aq}^{3+} + 2SiO_{2aq} + 8H_2O$

Boehmite precipitates first after the anorthite/dmisteinbergite dissolution due to its very low solubility.

$Al_{aq}^{3+} + 2H_2O = AlO(OH)_s + 3H^+$

The precipitated boehmite may be very fine-grained and porous; it may also contain silica in its composition as contamination from anorthite (Munz et al., 2012; Murakami et al., 1998). Such

modified boehmite covers plagioclase grains, slowing their further dissolution. The next phase that precipitates out of solution is calcium carbonate, which has a higher solubility than boehmite. Finally, kaolinite precipitates in the reaction between aluminum and silica.
However, in the case of the well-exposed samples, formulations included sodium-based activators. This allowed for the formation of mica-type minerals (paragonite, margarite, and muscovite) rather than kaolinite. Moreover, alkaline ions were likely found in the well environments, since even the formulation of #80/Silica that did not have any activator had potassium in its composition (in the unnamed zeolite).
Anorthite/dmisteinbergite phases persisted in all the tested CAC-based formulations, possibly with the partial carbonation causing fine-grained modified boehmite precipitation around these crystals. This nanoscale, fine-grained boehmite was likely not detected by the XRD measurements. Such an amorphous phase was visible in the #80/Silica sample around partially decomposed boehmite crystals after the 3-month exposure. The originally formed boehmite, on the other hand, disappeared in all the formulations except CAP#71/FAF. It is not clear why one of the CAC-based formulations preserved crystalline boehmite after the 9-month exposure but not the others.
Based on the TGA analysis, the amount of calcium carbonate formed in each blend depended on its calcium content. For the CAC-based formulations, it decreased in the following order: CAP#50/FAF > CAP#71/FAF = TSRC > #80/Silica. The calcium carbonate content of these blends slightly decreased over time (9-month vs. 3-month data). This was likely due to the dissolution of some of the calcium carbonate through continuous carbonation and the formation of calcium bicarbonate. The decrease in calcium carbonate was 18% for CAP#50/FAF, 15% for #80/Silica, and 12% for TSRC. CAP#71/FAF decarbonation weight loss did not change. Most importantly, unlike in the case of CSH-60/40, CAC-containing formulations still preserved stable crystalline phases, such as mica-type and plagioclase minerals, after the partial carbonation of the matrix. These phases included minerals from the mica family and the end member of the plagioclase series, albite. Moreover, carbonation of calcium–plagioclase minerals (anorthite and dmisteinbergite) was only partial over the experimental period. These allowed for the preservation of the mechanical and physical properties of the CAC-based formulations. Carbon fibers tested as part of cement compositions in the well for 9 months preserved their physical integrity, contributing to the samples' strength and toughness.
It should be noted that all material analyses were conducted at room temperature after exposure to HTHP conditions. In future work, in-situ material characterization and measurements of their mechanical properties under well conditions would be beneficial.

2.1.4. Gibbsite cement

A new aluminum-based, calcium-free cement was tested in the field exposure tests (formulations 9, 10, 11, 12 in chapter 2.1.5.1). This alkali-activated gibbsite cement (AGC) was originally designed for and evaluated under laboratory supercritical conditions (Pyatina & Sugama, 2023; Sugama & Pyatina, 2022). It is of interest as a standalone cementitious system that meets cement requirements for geothermal wells (strength above 1000 psi) while being highly flexible, but also as a part of other possible formulations with mineral compositions including aluminum, which are stable under HT geothermal well conditions. Most of the geological phases that survive in such environments are aluminum-rich and calcium poor, which is very different from the currently used cementing solutions historically created for above the ground constructions. Investigation of aluminum-based cementitious formulations can provide useful information for design of new

geothermal materials. Performance of field-tested gibbsite-based formulations in field tests is discussed in more details in this chapter.
The compositions (in mass percent) of cement samples discussed in this paper are given in Table 1. Cement slurries were prepared by dry-blending all components, hand-mixing them with water amount that allowed to obtain comparable self-leveling properties and poring them into glass tubes (18 × 150 mm). The glass tubes were left at room temperature for 12 h. Then samples were exposed to an 85°C environment with a relative humidity of 99.9% for another 12 h. Finally, they were autoclaved at 300°C for 12 more hours in a non-stirred Parr Reactor 4622. After the 300°C autoclaving, each tube was cut into 3 cylinders of ~40 mm each, and the solidified cement samples were removed from the glass before shipment to the wellsite for well-exposure tests or conducting mechanical properties tests. Evaluated gibbsite cement formulations are shown in Table 10.

Table 10. Compositions of AGC samples exposed in Newberry well in mass percent. The concentrations of SMS, MCF, and Zr are given in mass percent by the total mass of ($Al(OH)_3$, CAC#80, and SiO_2).

Sample name	**$Al(OH)_3$**	**CAC#80**	**SiO_2**	**SMS**	**MCF**	**Zr**	**Water**
AGC/MCF	60	-	40	5	10	-	51.6
AGC/Zr/MCF	60	-	40	5	10	10	51.6
AGC/CAC#80	50	10	40	5	-	-	44
AGC/CAC#80/MCF	50	10	40	5	10	-	51.6

2.1.4.1.Mechanical properties and water-fillable porosity

Compressive strength and Youngs modulus of 300°C-autoclaved and 9-month well exposed samples are shown in Figure 22. All the samples survived the 9-month exposure tests with only minor changes in strength and modulus. The strength slightly decreased for AGC/MCF samples with and without Zr (~12% strength decrease), persisted for the AGC/CAC sample, and increased for AGC/CAC/MCF sample (~40% increase). The changes in the modulus mirrored those of the compressive strength with the modulus after the exposure remaining in the desirable moderate range around 1000 MPa for all the formulations except the AGC/Zr/MCF one where the value of the modulus declined to 600 MPa. Such moderate values of the modulus even after the long well exposure times are uncommon for cementitious composites and indicate that ductility of the systems can persist in an HT well.
Interestingly the toughness of all the tested formulations noticeably improved after the exposure. Toughness is a combination of strength and ductility and is a very desirable property for geothermal cements. Because of the high ductility of these formulations their average toughness was relatively high even before the exposure tests despite their moderate strength (0.29 N*mm/mm3). Their average toughness further increased by stunning ~240% after the exposure reaching 0.97 $N*mm/mm^3$ (Figure 23).
The high ductility of these formulations is partially due to their relatively high porosity of about 50%. Porosity of the samples after exposure decreased by nearly 6% with the largest decrease experienced by the AGC/CAC/MCF sample. The porosity of that formulation dropped to ~48%.

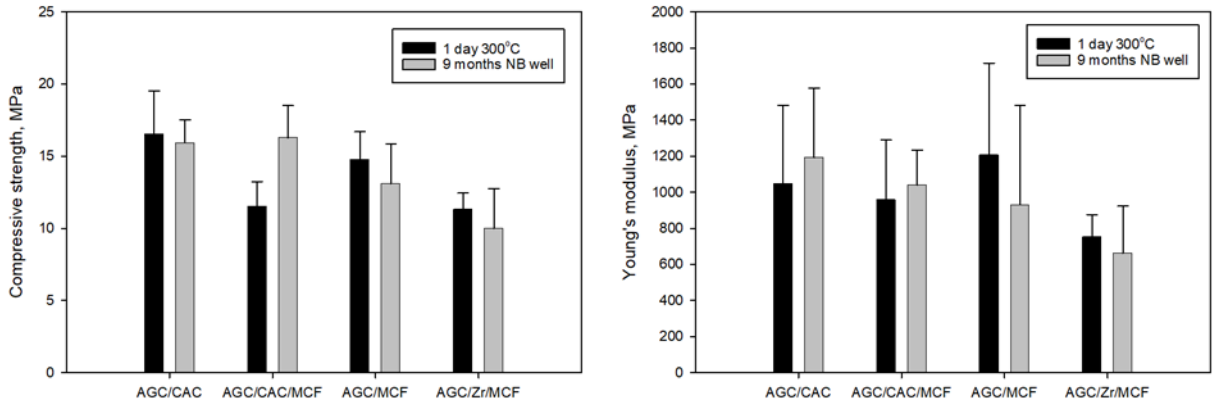

Figure 22: Compressive strength and Youns's modulus of 300ºC autoclaved and 9-month well exposed samples.

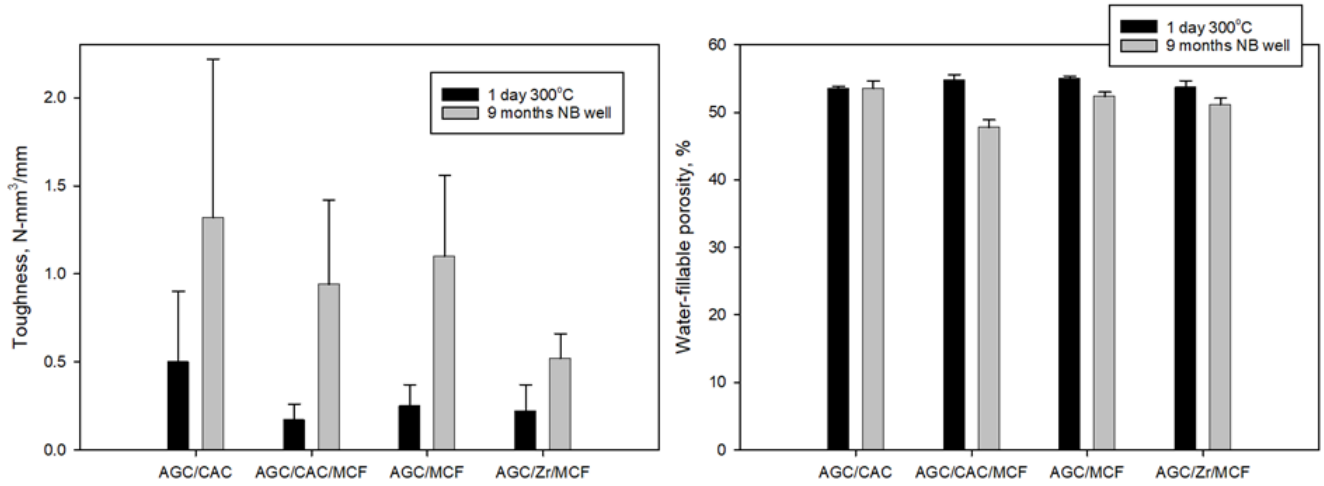

Figure 23: Compressive toughness and water-fillable porosity of 300ºC autoclaved and 9-month well exposed samples.

Noticeably, increase in compressive strength and porosity decrease after the 9-month exposure did not compromise high ductility of these formulations.

AGC and AGC/Zr formulations were tested under supercritical conditions earlier (Pyatina & Sugama, 2023). They both showed decreased strength (~20% decrease) and increased porosity (~10%) after 30 days under supercritical water. These performance differences could be partially attributed to the difference in exposure times (months of supercritical conditions were not feasible in the laboratory tests). It could also be the effect of the well fluid environment, which was not pure water as in the laboratory tests. CMF used in the case of the field-exposed samples and absent in the laboratory supercritical tests are chemically inert and could not change samples' compositions. To better understand mechanical behavior of the samples phase analyses were undertaken to elucidate compositional changes in the well-exposed samples.

2.1.4.2. Phase compositions

Crystalline phase compositions

The crystalline phase compositions of the tested samples are shown in Figure 24. There is no difference between the patterns of the samples with and without MCF and Zr. In fact, albite was the major phase in all three samples. In the case of AGC with CAC albite/anorthite formed (ICDD number 04-024-2151). Most of the other high-intensity peaks were attributed to paragonite and halloysite (ICDD numbers 04-014-7680 and 00-058-2031). Since the patterns of these two phases strongly overlap it is difficult to say whether both or only one of them was actually present in the samples. All samples showed some silica peaks and the samples with CAC also had small peaks of HT zeolite analcime commonly reported in the alkali-activated formulations with CAC. It was also observed in another alkali-activated formulation of CAC after the 9-month Newberry well exposure (Pyatina et al., 2024). In nature albite can undergo metasomatic replacement by sodium-rich nepheline and sodalite (Drüppel & Wirth, 2018). Some nepheline was also discovered in the samples after the 9-month exposure (ICDD number 00-019-1176). Paragonite is generally stable at these temperatures and if it breaks, it forms albite and corundum (Chatterjee, 1970). Thus, the formation of albite, nepheline, and paragonite was consistent with the samples' compositions and the expected formation of HT minerals under the well conditions. The sample modified with Zr, contained vlasovite mineral (ICDD number 04-016-5105) suggesting some reactivity of added Zr over the exposure period.

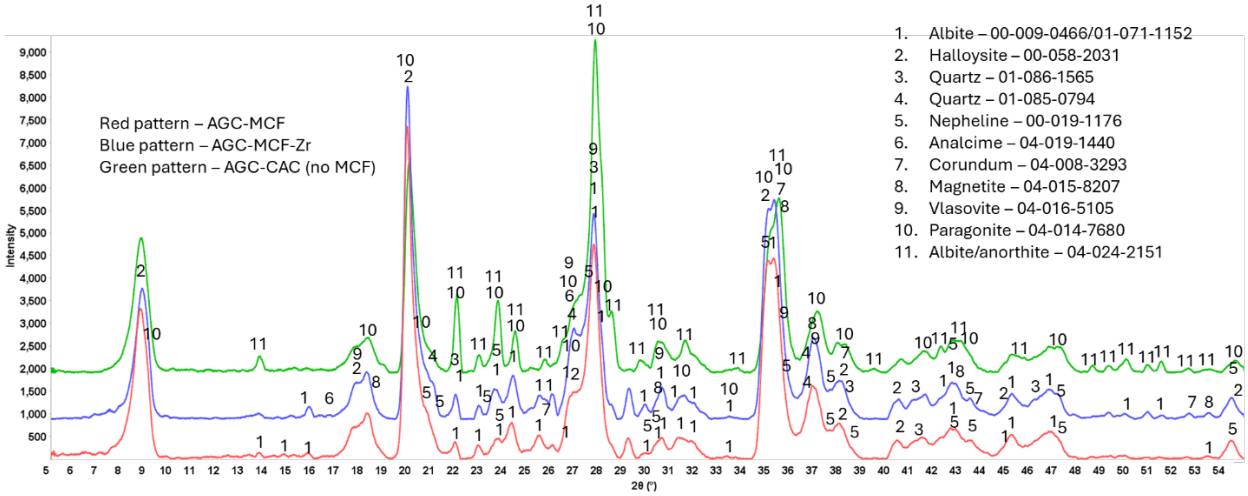

Figure 24: Crystalline phase compositions of the three tested AGC formulations after the exposure in Newberry well for 9 months.

Interestingly, crystalline boehmite was not detected in any of the samples. Aluminum was reacting with silicon with formation of albite and paragonite in these samples with a silica source. Likewise, the initially formed boehmite disappeared in other highly alkaline formulations after the 9 months in the well (Pyatina et al., 2024). The only formulation where boehmite persisted had noticeably lower pH of the slurries (phosphate cement). Boehmite transition to gamma aluminum hydroxide during thermal shock tests was observed in our previous work with alkaline-activated calcium-aluminate/fly ash F blend (Sugama & Pyatina, 2018).Boehmite is not necessarily the most desirable binding phase, it is compressible due to its layered structure with hydrogen bonds. But it is

carbonation resistant and provides high material ductility. Nevertheless, although crystalline boehmite was not detected in the AGC samples, all the phases present in them resisted the carbonation that compromised OPC/silica formulation mechanical properties. This was reflected in the absence of crystalline carbonate peaks in the XRD patterns.
For the samples cured under supercritical conditions for 30 days boehmite, paragonite, as well as small amounts of analcime were detected. On the other hand, the end member of the Feldspar mineral series, albite, or its decomposition product nepheline were not detected. These differences in the compositions suggest that mechanical properties of the samples can be explained by shorter curing time under supercritical conditions, so that the expected final phase compositions of the samples with boehmite transforming into albite in reactions with silicon were not reached.

Thermogravimetric analysis

The results of thermogravimetric and differential thermogravimetric analyses for AGC/CAC and AGC/MCF samples are shown in Figure 25. The major weight loss event for both samples occurred between ~450 and 650ºC (3.9 and 3.6% respectively for AGC/CAC and AGC/MCF). This range corresponds to the decomposition of boehmite or its polymorph diaspore. However, XRD patterns did not contain peaks of crystalline boehmite. So, the likely contributors to that weight loss are halloysite, which dehydroxylates to metahalloysite ~530-590ºC and albite that decomposes at ~650ºC (Feng et al., 2012). The AGC/CAC sample also had a small weight loss between ~270ºC and 500ºC (a shoulder). Zeolite, analcime, decomposes in that temperature range (Cruciani, 2006). The weight loss above ~700ºC corresponds to the decomposition of CMF. It was also observed in the AGC/CAC/MCF sample, the decomposition pattern of which was otherwise identical to that of AGC/CAC sample. The decomposition pattern of AGC/MCF/Zr sample was identical to that of AGC/MCF.

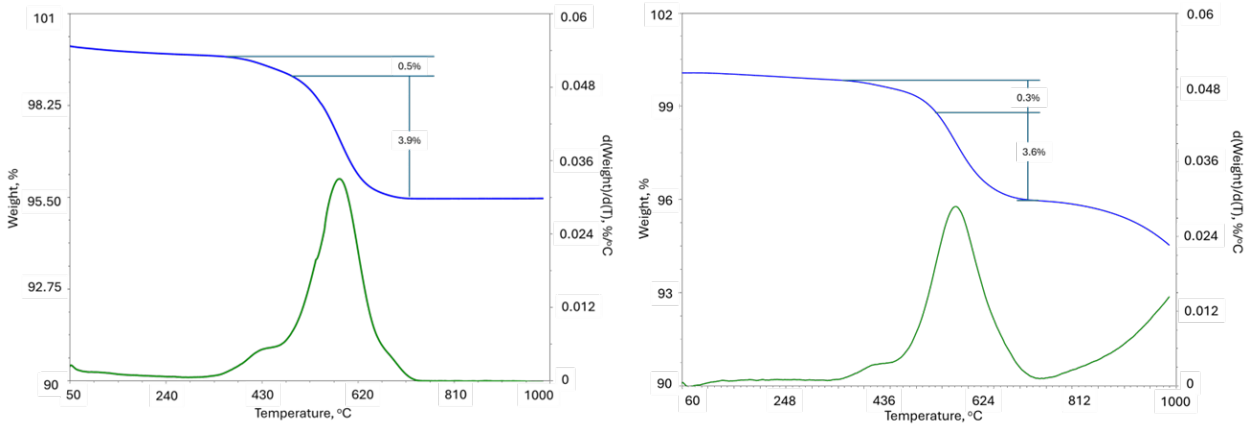

Figure 25: Thermogravimetric and differential thermogravimetric analyses of the AGC/CAC (left) and AGC/MCF (right) 9-month well exposed samples.

Morphologies of the exposed samples

Figure 26 shows photomicrographs and elemental compositions of typical sites of AGC/CAC samples exposed for 9 months in Newberry well. A flaky crystals morphology and elemental compositions of sodium deficient paragonite can be seen in locations 1 and 3. Smaller denser crystals with the typical albite/anorthite composition are seen in location 2.

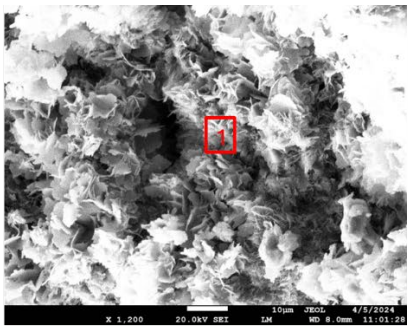

Spectrum 1			
Element	Wt%	Wt% Sigma	Atomic %
O	37.08	0.67	51.01
Na	2.33	0.21	2.23
Al	24.81	0.38	20.23
Si	29.08	0.44	22.79
K	4.93	0.31	2.78
Ca	1.76	0.20	0.97

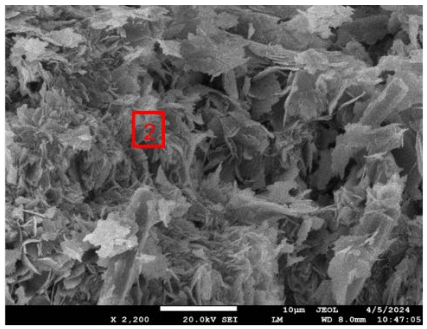

Spectrum 2			
Element	Wt%	Wt% Sigma	Atomic %
O	37.17	0.88	50.66
Na	5.28	0.32	5.01
Al	15.79	0.41	12.76
Si	37.98	0.67	29.48
K	2.63	0.48	1.46
Ca	1.15	0.28	0.63

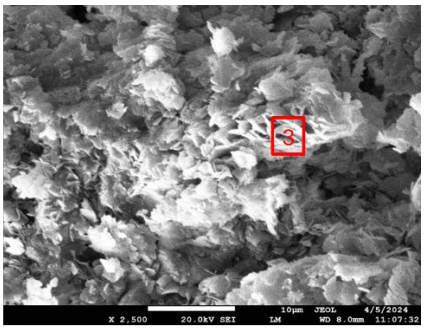

Spectrum 3			
Element	Wt%	Wt% Sigma	Atomic %
O	36.40	1.03	50.30
Na	2.03	0.32	1.95
Al	24.09	0.57	19.74
Si	30.84	0.69	24.28
K	4.59	0.61	2.60
Ca	2.05	0.36	1.13

Figure 26: Photomicrographs and elemental compositions of AGC/CAC 9-month well exposed sample.

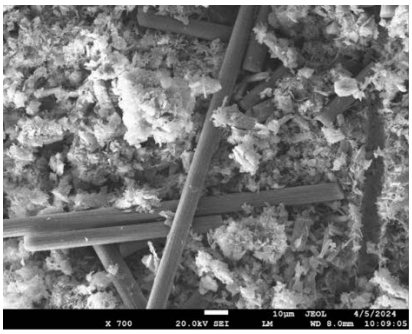

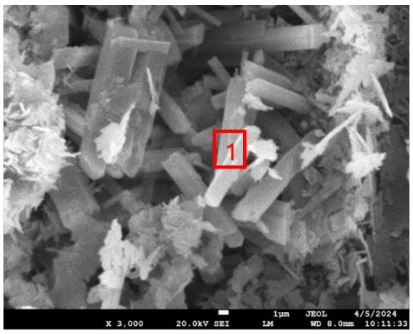

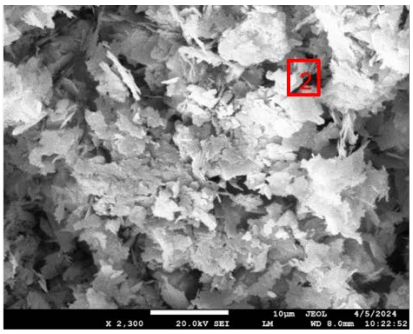

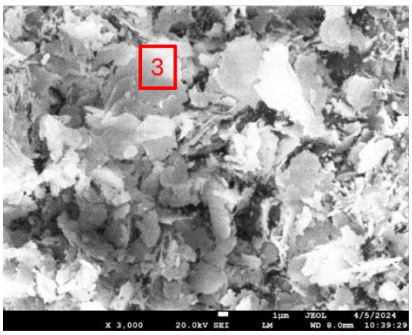

Spectrum 1			
Element	Wt%	Wt% Sigma	Atomic %
O	33.76	0.81	47.44
Na	4.87	0.28	4.76
Al	12.38	0.32	10.32
Si	41.29	0.62	33.05
K	7.70	0.43	4.43

Spectrum 2			
Element	Wt%	Wt% Sigma	Atomic %
O	31.98	0.89	45.15
Na	4.51	0.32	4.43
Al	15.79	0.39	13.22
Si	42.53	0.69	34.20
K	5.18	0.46	2.99

Spectrum 3			
Element	Wt%	Wt% Sigma	Atomic %
O	31.94	1.96	46.33
Na	1.94	0.59	1.96
Al	20.76	0.95	17.86
Si	29.77	1.22	24.60
K	15.60	1.53	9.26

Figure 27: Photomicrographs and elemental compositions of AGC/MCF 9-month well exposed sample.

Figure 27 shows photomicrographs and elemental compositions of typical sites of AGC/MCF well-exposed samples. Intact MCF can be seen in the lower magnification photomicrograph on the left. The fibers survived the 9-month exposure without any visible damage. The tubular crystals have a composition of halloysite, however, albite that has similar elemental composition can also crystallize as tubulars or flat and bladed crystals (site 2) (Christidis, 2011). Crystals in site 3 have flake-like morphology and elemental composition of paragonite.

The morphological features of the other 2 tested formulations were like the ones shown for AGC/CAC/MCF and AGC/MCF/Zr samples, with intact MCF, and crystals of paragonite and albite dominating samples' morphologies.
In summary, the morphological data agreed with the XRD results confirming presence of albite, paragonite and, possibly, halloysite. Also, in agreement with the XRD results boehmite crystals were not detected in the samples.

2.1.4.3. Discussion

Alkali-activated gibbsite based cementitious blends that are of interest as standalone systems or parts of other cementitious materials have some very attractive properties for EGS, including low or no calcium, providing its high carbonation resistance, and very high ductility, essential for applications in wells with frequent thermo-mechanical stresses. Their relatively high porosity can accommodate internal interstitial water expansion during the rapid well heating by the HT geothermal fluids. Tested under supercritical conditions (up to 30 days) and Newberry well (up to 9 months) they showed somewhat different changes of properties, with the strength decrease and porosity increase in the first case and varied strength response that depended on the formulation but without any significant strength decrease and porosity mostly decreasing in Newberry tests. Importantly, unlike most of the cementitious composites that experienced stiffening after longer exposures to high-temperature conditions gibbsite cement increased its toughness on average by 240% after the 9-month exposure to 325-350ºC Newberry well environments without any significant increase in stiffness. High cement ductility ensures a large safety operational envelope of cements decreasing the probability of cement failure under the thermal shock conditions typical for geothermal wells (Meng et al., 2024). The fact that gibbsite cement does not stiffen after 9 months of HT exposure is remarkable. Currently, the general strive for well integrity is to increase ductility or/and allow some casing movement during the stresses of the systems exposed to supercritical conditions (Thorbjornsson & Kaldal, 2021). The flexibility of the casing allows avoiding metal breakage under large thermal stresses. However, movements of the cemented casing will necessarily break the cement sheath if cement ductility and the magnitude of the casing movements are mismatched. Cement ductility can be increased by foaming it or adding fibers. However, for the large thermal stresses foam may not be appropriate, since gas expansion during heating will damage foam cement that is generally noticeably weaker than regular cement formulations and is unlikely to be able to withstand large gas expansion. For these reasons, AGC's remarkable ductility is very attractive for wells under large thermal stresses. This property of AGC can be seen in Figure 28 that compares stress-strain curves of phosphate-based cement, OPC/silica formulation and AGC after a day of 300ºC curing. While currently used OPC- and phosphate-based formulations reach high stress before the fracture, their abrupt fracture is typical for brittle materials. The AGC formulation, on the other hand, exhibits very ductile behavior with a long displacement tail under compression.
Under elevated temperatures AGC formulations undergo some phase transitions that take time. Incomplete phase transitions under the shorter period of supercritical exposures can account for the difference in mechanical properties of the samples cured at 400ºC and those exposed in Newberry well. Longer curing times causing boehmite decomposition, aluminum reactions with silica with formation of paragonite and albite were observed in the field exposed samples. Small nepheline peaks in these samples suggest a possibility of further albite transition into nepheline or nepheline formation from aluminum from decomposing boehmite. Clay minerals, observed as the decomposition products of feldspars by water saturated with carbon dioxide in nature, and found

in the AGC after the well exposure tests, including paragonite and halloysite, ensure consistent performance of this blend and its carbonation resistance. The tubular and flaky morphologies of the samples can explain their high toughness and low stiffness.

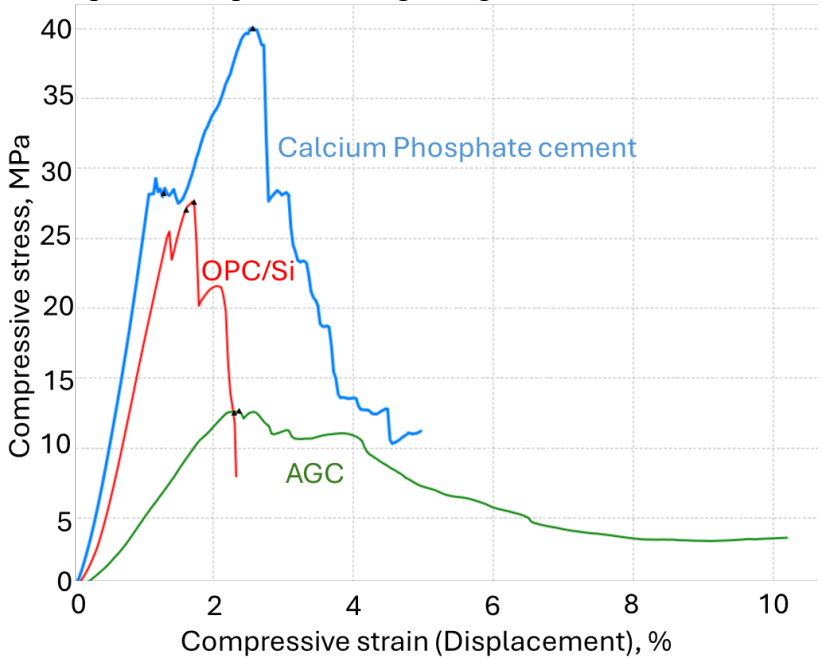

Figure 28: Comparison of typical stress-strain compressive curves for OPC/silica, phosphate cement, and AGC formulations after a day of curing at 300ºC.

Nevertheless, whether AGC with its high porosity and very low stiffness can withstand large thermal shocks and provide good corrosion protection of the metal casing remains to be seen. Good metal-cement bond and low cement permeability are necessary in addition to the resistance to acidic environments for the metal protection in EGS. Higher porosity cements that are great to accommodate thermal shock conditions (e.g. foam cements) are generally less favorable for metal corrosion protection.

2.1.5. Conclusions on the field exposure tests

The performance of various cementitious composites was evaluated in HT geothermal well exposure tests and compared against that of the OPC/silica blend. The tested formulations included calcium–aluminate cement (different grades) blends with silica or fly ash F. Some of the blends had alkali (SMS in TSRC) or chemical activators (SHMP in CAP cement blends). Additionally, blends reinforced with CMF were tested in 9-month field exposure tests.

The results of the tests at ~350 °C showed that CAC-based blends outperform the reference OPC/silica one. Interestingly, the findings of the short-term (3-month) and long-term (9-month) exposures to the Newberry well conditions differed in an important way. The short-term exposure increased the shear and tensile strength of most of the tested formulations, including the control OPC/silica one. Calcium phosphate cement formulations, however, experienced a slight reduction in shear and no change in tensile strength (Pyatina et al., 2024). This loss was recovered after the 9-month exposure. On the other hand, the 9-month exposure led to a very substantial loss of strength, stiffness, and toughness for the OPC/silica blend. This happened because of the fast degradation of calcium–silicate hydrates through carbonation, resulting in compromised

mechanical properties. The extent of partial carbonation in the CAC-based blends depended on their calcium content. The carbonation took place through the removal of calcium from plagioclase end-series member anorthite (dmisteinbergite) and the formation of the end-family member albite and mica family minerals margarite, muscovite, and paragonite. These mineral phases allowed for the persistence or improvement of the mechanical properties of the samples during their well exposure. Carbon microfibers persisted in cementitious composites through the 9-month exposure without any visible degradation, improving their strength and toughness.

AGC is an attractive material for EGS applications due to its high toughness and great carbonation resistance. The results of supercritical and field exposure tests showed that AGC meets geothermal well strength criteria, with the mechanical properties and cement ductility persisting after long-term (9-month) exposure to high-temperature, high-carbonate concentration conditions in a geothermal well. The phase transitions taking place in the cement over long periods at high temperature result in boehmite reactions with silica with formation paragonite, halloysite, albite, nepheline mineral phases. Boehmite persisted during shorter (30-day) exposures to supercritical conditions in laboratory experiments. Further AGC modifications may be needed to decrease its porosity, currently nearing 50%, and to ensure its ability to provide good steel corrosion protection.

2.2. Work on cement formulations for fire flood wells

The conditions of fire flood wells that could be candidates for the applications of thermal shock resistant cement (TSRC) were defined in collaboration with CUDD Energy Services. In these wells cement is pumped under the ground at room temperature, left to harden for a week or two, and then heated to ~ 375^{o}C through casing with a heater. The heating is done in a central well surrounded by several peripheral wells, so that the heat radiates to the peripheral four wells. After oil starts flowing the heater is removed and temperature is controlled by the addition of nitrogen to the wells. The drop in temperature may be as much as 300^{o}C in 8 hours. Additionally, to improve heating conditions the wells are flooded with cold water through the casing at some intervals. TSRC blend developed to withstand thermal shock conditions while keeping good bonding with carbon steel was tested for high-temperature geothermal wells. Its set and curing were performed at 200-350^{o}C. In the case of fire flood wells cement solidification takes place at room temperature. Several types of cements were evaluated for fire flood wells: 1) TSRC (#80/FAF – 60/40 mass ratio and 6% SMS by the weight of blend), 2) TSRC modified with different calcium-aluminate cement grades (CACs), 3) TSRC with fiber re-enforcement (each at 5 mass % by weight of blend), 4) Calcium-phosphate (CAP) cement with fast-set CAC#71) CAP cement with metakaolin and silica, 6) Fast-set CAC #71 alone, 7) CAC with metakaolin and silica, 8) Class H cement with metakaolin and silica. Unless it is stated otherwise all the formulations were set at room temperature for 3 days and then exposed to 400^{o}C heat for another 3 days.

The results of the tests are shown in Figures 28-35.

As expected, after 3 days of curing under room temperature none of the TSRC formulations reached 1000 psi compressive strength. For the non-reinforced cement, the strength was the highest with CAC#80 (~600 psi). For grades #50, 71, and Fondu the strength was below 200 psi. Addition of carbon fibers to TSRC with #80 increased the strength above 700 psi, modification of the blend with glass fibers decreased its strength, and the combination of the fibers showed an intermediate strength development (Figure 28). After heating at 400^{o}C for 3 days the strength increased for all non-modified blends but decreased for #80-based blend with the fibers. The Young's modulus

results mirrored those of compressive strength. Except noticeable modulus decrease for the blend with carbon fibers (Figure 29).

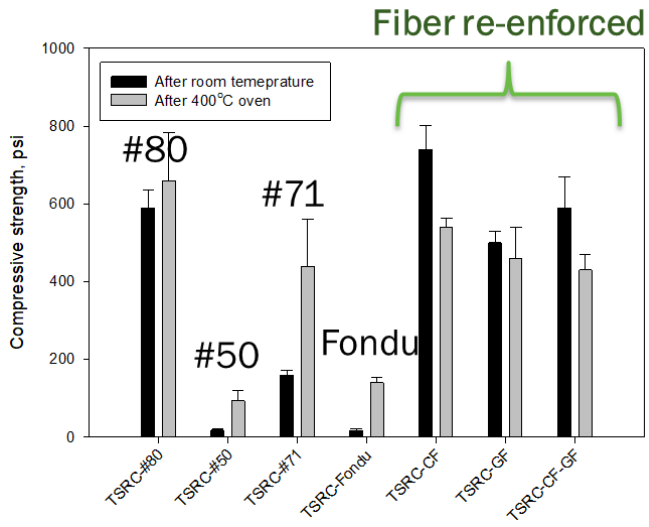

Figure 28. The compressive strength of TSRC with different CAC grades and reinforced with carbon fibers (CF, 5% by weight of blend), glass fibers (GF, 5% by weight of blend), and both CF and GF (5% by weight of blend each) after 3 days at room temperature and 3 days 400°C heat exposure.

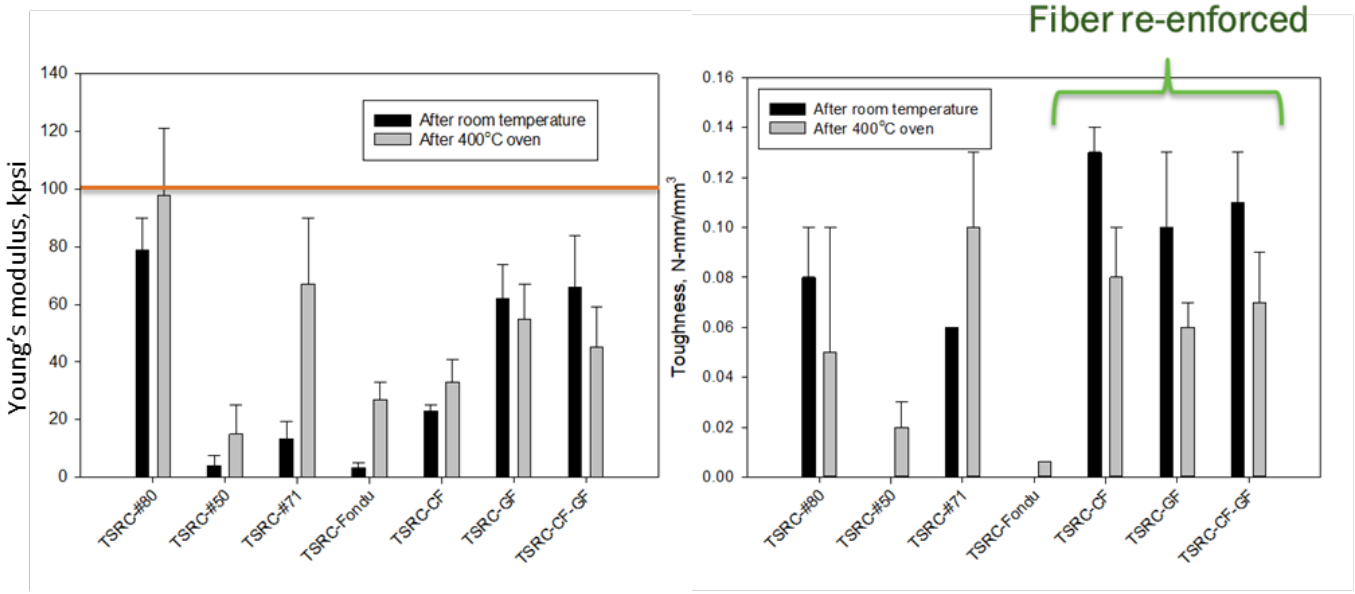

Figure 29. The Young's modulus and toughness of TSRC with different CAC grades and reinforced with carbon fibers (CF, 5% by weight of blend), glass fibers (GF, 5% by weight of blend), and both CF and GF (5% by weight of blend each) after 3 days at room temperature and 3 days 400°C heat exposure.

The toughness was low for all the blends due to their low strength. The toughness of fiber-modified blends noticeably decreased after the heat conditions because of the cracks and fissures forming in the samples.

These tests demonstrated that 1) to develop short-term mechanical properties TSRC needs to solidify at temperatures above the room temperature; 2) HT heating of room-temperature solidified TSRC will improve its strength unless modified with fibers; 3) carbon and glass fibers do not improve performance of TSRC solidified at room temperature and heated to 400ºC but cause material cracking. It was of interest to see whether longer initial curing of the cement allows it to develop mechanical properties, since the fire flood wells may be left for weeks before the heaters are introduced. The strength development in TSRC formulations after nearly 2 weeks (13 days) at room temperature was evaluated. These tests were performed with TSRC modified with carbon, glass fibers or both (Figure 30).

The blends developed more than 1000 psi compressive strength after 13 days at room temperature. However, all mechanical properties strongly degraded after the 400ºC heat exposure. The likely reasons for it were fiber-reinforcement degradation as was seen in the short-term tests, but more importantly, phase transitions from low temperature phases to high temperature compositions under the heat conditions.

In summary, the use of TSRC in fire flood wells with room temperature cement solidification conditions is possible but not very interesting due to either limited development of the mechanical properties after a short room temperature curing or formation of undesirable low temperature phases after longer (~2 weeks) of curing. For the blend to develop adequate properties the wells would probably need to be heated to more than 60ºC to avoid formation of low temperature hydrates.

We also evaluated the performance of other CAC-based cements under these conditions.

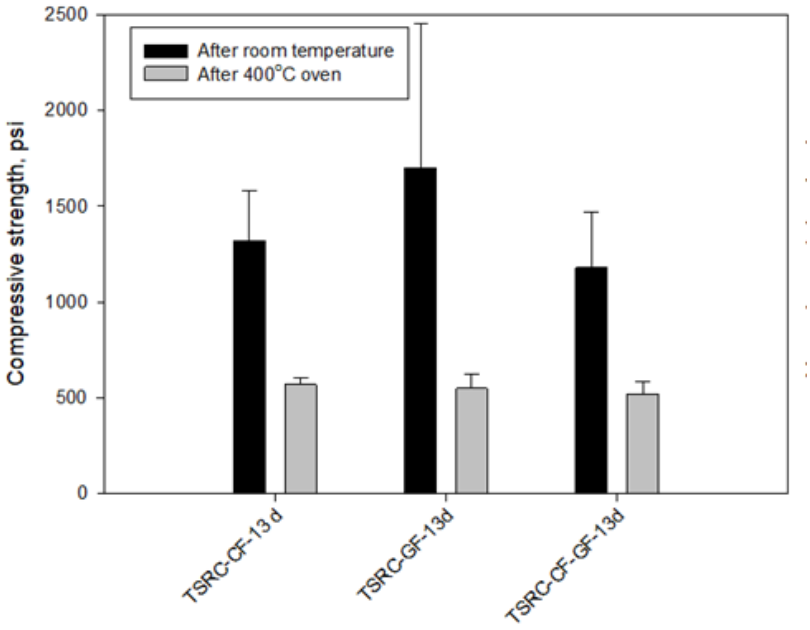

Figure 30. The compressive strength of TSRC reinforced with carbon fibers (CF, 5% by weight of blend), glass fibers (GF, 5% by weight of blend), and both CF and GF (5% by weight of blend each) after 13 days at room temperature and 3 days 400ºC heat exposure.

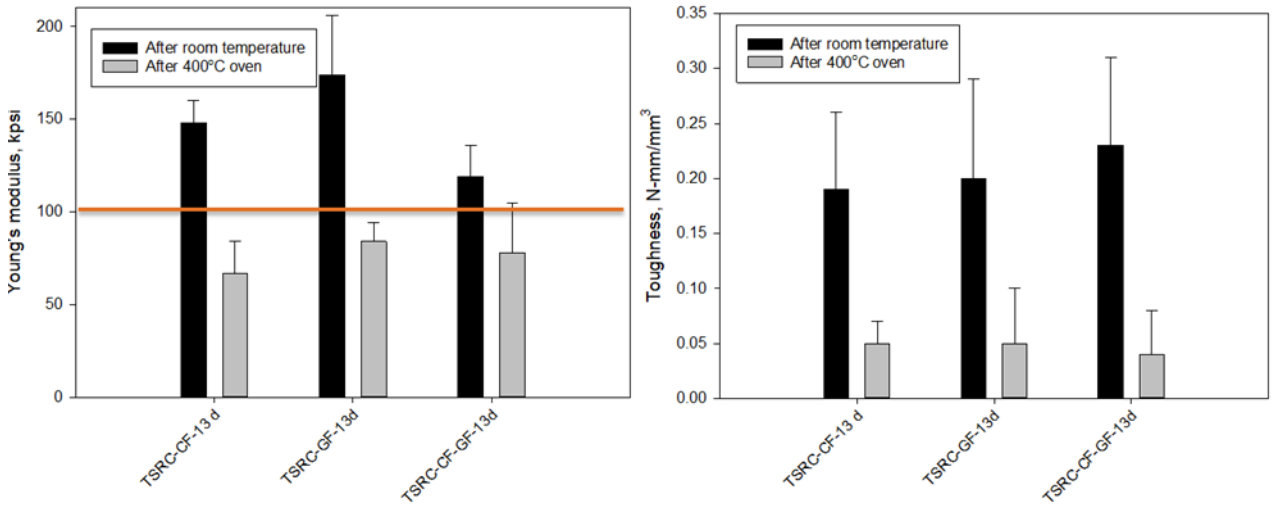

Figure 31. The Young's modulus and toughness of TSRC with different CAC grades and reinforced with carbon fibers (CF, 5% by weight of blend), glass fibers (GF, 5% by weight of blend), and both CF and GF (5% by weight of blend each) after 13 days at room temperature and 3 days 400°C heat exposure.

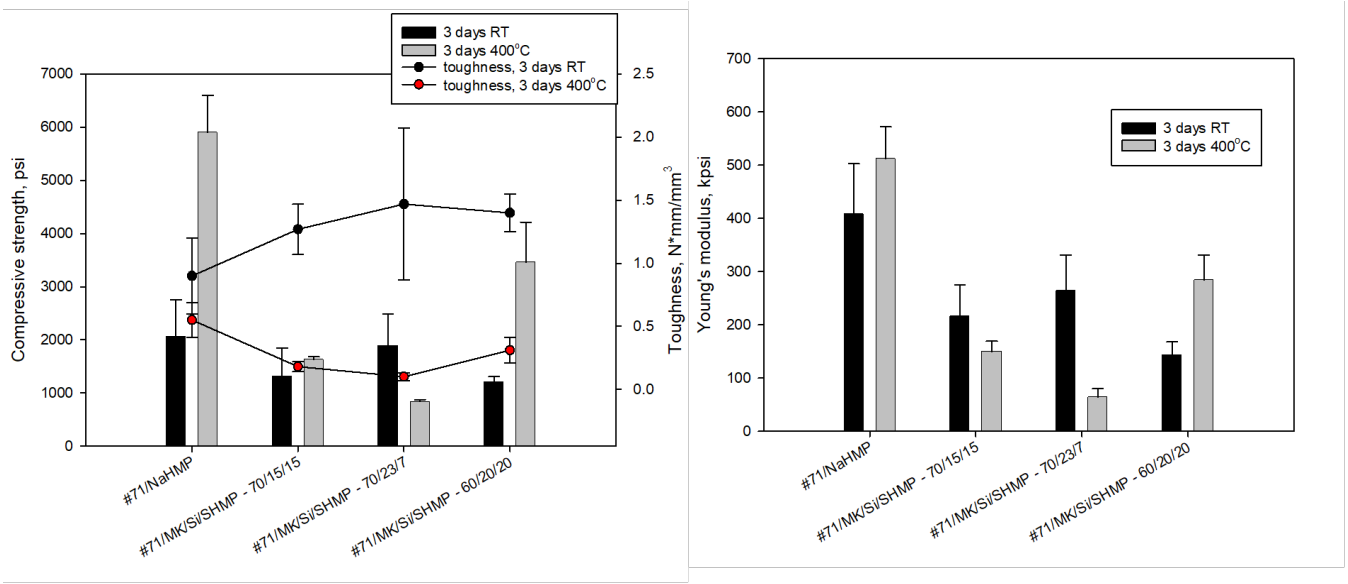

Figure 32. The compressive strength, Young's modulus, and toughness of calcium phosphate (CAP) cement after 3 days at room temperature and 3 days 400°C heat exposure.

Calcium phosphate (CAP) cement is known to quickly develop mechanical properties due to the fast chemical reactions between calcium ions from CAC and phosphate ions from SHMP. We evaluated the performance of that cement for fire flood well applications. CAP cement was formulated with CAC#71 that provides fast set alone or in blends with silica flour and MK. SHMP was added at 6 mass% of the cement or blend (Figures 32 and 33). As expected, all the tested formulations developed more than 1000 psi compressive strength after 3 days at room temperature (Figure 32). The strength and brittleness decreased with the decreased amount of #71 in the blend,

increasing cement toughness on average by more than 50% to values above 1 N*mm/mm^3. The Young's modulus for #71/SHMP formulation was very high, in the brittle failure region (>400 kpsi), for the formulations modified with silica and MK the moduli were around or below 200 kpsi, the values that indicate moderate failure mode. The strength after the heating dramatically increased for the #71/SHMP formulation from 2060 to 5900 psi. With the cement becoming even more brittle (the modulus value 512 kpsi). The toughness of that formulation decreased by nearly 40%. The samples cracked after they were removed from the oven. The two other formulations that have the problem of cracking after the heat exposure were #71/MK/Si/SHMP – 70/15/15 and 70/23/7. The #71/MK/Si/SHMP -60/20/20 formulation formed some bubbles, but no cracks. The strength of that formulation nearly tripled but the toughness dramatically decreased from 1.4 to 0.15 N*mm/mm^3. The modulus was nearly 300 kpsi. The performance of that formulation was the best under the test conditions.

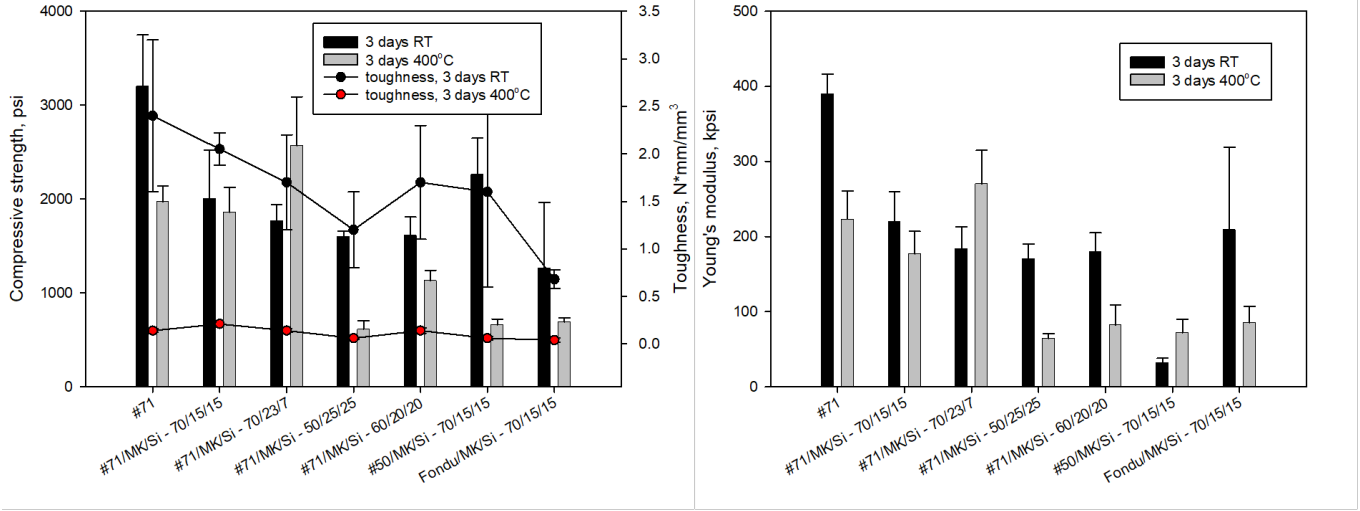

Figure 33. The compressive strength, Young's modulus, and toughness of various calcium aluminate cements after 3 days at room temperature and 3 days 400ºC heat exposure.

CAP cement formulations with more cost-effective CAC#50 and Fondu (70/30 bends with FAF) developed very low strength of 340 and 500 psi after the 3-day room-temperature curing. The strength of #51 CAC blend increased to 2450 psi after the heat, the modulus was in the acceptable moderate failure range (~190 kpsi). but the toughness of the cement was very low at 0.28 N*mm/mm^3.

Formulations of CAC alone (#71) and modified with silica and MK (#71, #50, Fondu) were tested for fire flood well applications. Formulations with #71 developed high room temperature strength, but most of them cracked after being removed from the heat. The three formulations that did not crack included those that did not develop very high initial strength – blends with CAC#50, Fondu, and #71/MK/Si (60/20/20). However, the strength of these blends strongly declined after the heat (Figure 33). All the heat-exposed blends lost their toughness, that was very high (above 1 N*mm/mm^3) after the room-temperature curing. The Young's modulus of the blends that did not crack after the heat was very low (below 100 kpsi). In combination with the low strength this produced low toughness. For other blends, the addition of silica and MK clearly decreased the strength of CAC#71 but when 30% of the cement was replaced the strength after the heat persisted. For high cement replacement strength losses were observed.

In summary, CAC-based cement formulations, including CAP cement showed fast strength and toughness development at room temperature. Toughness decreased for all tested formulations after the heat. Many formulations cracked when being removed from the oven, resulting in decreased strength. Modifications with MK and silica/MK of some CAP and CAC-alone-based formulations allowed persistence of strength after the heat exposures. Between 30 and 40% of cement replacement with silica/MK showed the most promising results for the strength persistence in heat exposure tests.

Based on the positive results of MK addition to CAC-based formulations we ran some additional tests with formulations based on OPC, class H. Class H cement formulations were tested for 3 and 7 days of room-temperature curing followed by 3 days in a 400ºC oven (Figure 34). The cement was tested with silica (60/40 mass ratio) and partial silica replacement by MK (H/MK/Si-1 – 70/15/15 blend mass ratio and H/MK/Si-2 – 70/27/3 mass ratio; H/MK – 70/30 mass ratio). None of the blends developed the target 1000 psi strength in the first 3 days of curing. The blend with 27% of MK developed strength of 920 psi. However, the strength of that blend did not increase after 7 days of curing, while the blend with silica flour and with 70/15/15 H/Si/MK ratio reached the target in 7 days. The strength of all the blends except the H/MK one increased after the heating with the blends that included MK exceeding 1500 psi. The blend of H/Si strength remained around 1000 psi both after the 7-day room-temperature curing and after the heating. And the blend of H/MK did not reach the target either after room temperature curing or after the heating. This blend was not tested for 7 days. The Young's moduli of all the blends remained in the desirable moderate brittleness range after the heating.

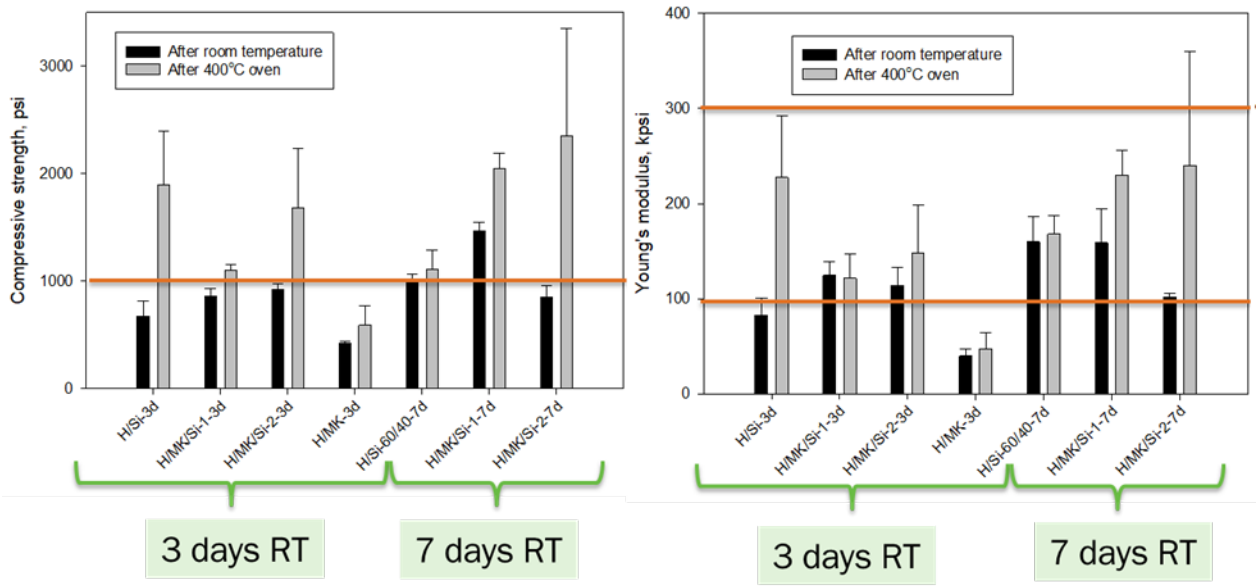

Figure 34. The compressive strength and Young's modulus of class H, OPC, silica, and MK blends after 3 and 7 days at room temperature and 3 days 400ºC heat exposure.

The toughness was noticeably higher for the blends with MK after the first 3 days of curing (Figure 35). However, after 7-days of curing, as cement hardened, its strength and modulus increased, and the toughness dropped. For the 3-day room-temperature cured cements the toughness also dropped drastically after the heat treatment. This is surprising because for some of these formulations, e.g.

H/MK/Si-1 (70/15/15) and H/MK, the strength and modulus developed after 3 days at room temperature did not change significantly with the heating, but their toughness dropped. The low toughness of the reference formulation after 3 days at room temperature remained low after the heating. The toughness of all tested formulations was low after 7 days at room temperature, although it was nearly double for the one with partial silica replacement by MK. The heating did not affect the toughness of these formulations.

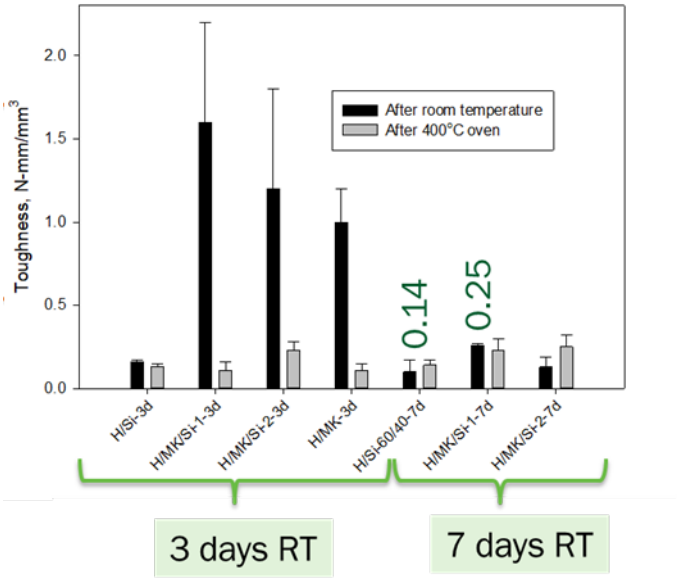

Figure 35. The toughness of class H, OPC, silica, and MK after 3 and 7 days at room temperature and 3 days 400ºC heat exposure.

In summary, OPC-based formulations performed reasonably well under the test conditions. It is likely that increase in their strength during the heating was caused by the carbonation in the oven, which was shown in a short time to have a positive effect both on OPC strength and porosity, increasing the first one and decreasing the second (Pyatina et al., 2024). The decrease of toughness after the heat exposure was similar for OPC and CAC-based formulations.

2.3.Set retardation of TSRC

Retardation of chemically activated cementitious composites is difficult. Fast reactions of chemical phosphate cement caused premature material solidification in several field jobs (personal communications with service companies). Solidification control of alkali-activated cementitious materials remains one of the main obstacles on the way of their field applications at elevated temperatures. Cement hydration reactions involved in the formation of solid phases are generally exponentially accelerated with the temperature increase. Set retarders are expected to provide controllable and predictable time of composites solidification when pumping cannot be pursued any longer, while not delaying or compromising development of desirable mechanical properties after the placement is completed. Although, for the most part, geothermal wells are cooled by fluids circulation before cementing, slurries of composites may have to remain pumpable for more than 6 hours at temperatures up to 230ºC. Acidic retarders have been reported to be effective for chemical phosphate-based cements, however, the setting time response to the retarder concentration is highly non-linear with little set delay at lower retarder concentrations followed by exponential setting time increase at higher ones (Mac et al., 2014). Neither poor nor strong response of setting time to retarder concentration is desirable – the first one requiring high retarder

amounts, the second one making it difficult to accurately control the setting. In our earlier work TSRC was successfully retarded with tartaric acid up to 100ºC (Pyatina et al., 2016). But for HT EGS wells 5 hours of pumping time may be insufficient for secure cement placement and the placement temperature can be significantly higher than 100ºC. Retardation of highly alkaline alkali-activated materials (AAMs) has been reported only at low temperatures (Li et al., 2023). Control of AAMs' solidification reactions remains a major challenge.

There are several general strategies to slow down solidification of AAMs by interfering with either dissolution or condensation reactions taking place during the activation-solidification process. These include changing the precursor compositions, alkali activators, water content, or adding retarders (Dai et al., 2020; Kamath et al., 2021; Liu et al., 2017; Tong et al., 2021). Dilution of reactive aluminum-silicates with less reactive clays and mica minerals, partial replacement of Al^{3+} by Fe^{3+} in $Na_2O(CaO)$-Al_2O_3-SiO_2 systems, decrease of calcium content and increase of the Si/Al ratio, which makes activation-condensation reactions more susceptible to the effects of retarders, increase of the reactants particle size, alternative chemistries of alkali activators, and decreased alkalinity, all may be considered as strategies for slowing down solidification of the composites (Li et al., 2023).

Chemical retarders that may alter dissolution of the precursors, nucleation, and growth of reaction products have shown some promise for alkali-activated cement-free systems at low temperatures. These retarders include phosphorus-, boron-, zinc-based additives and organics such as sucrose and carboxy-methyl cellulose (Sugama & Pyatina, 2015; Tong et al., 2021). The advantage of boric acid/borax and phosphoric acid/phosphate as retarders is that they do not compromise the development of mechanical properties when added in limited amounts and are stable at HT (Tong et al., 2021).

Experimental work to delay solidification of TSRC was done at BNL using calorimetric studies, where cement hydration heat release can indicate cement set times. However, for the most part, these experiments were performed with cement slurries mixed by hand (low shear conditions) and under static conditions at 85ºC. API 10B standard requires pumping time to be determined in thickening time tests, where slurries are prepared under high shear conditions in Waring blender. After the Warring blender mixing the slurries are subjected to a continues low shear in a consistometer while their consistency (related to viscosity) is monitored. CUDD Energy conducted standard consistometer tests on formulations recommended by BNL.

Based on the results of calorimetric measurements BNL recommended retarder composition for thickening time tests performed by CUDD Energies. The composition of TSRC was as follows unless mentioned otherwise: CAC #80: 60 wt%, FAF: 40 wt%, SMS: 6% by weight of CAC and FAF blend. All retarders were obtained from Sigma-Aldrich.

Figure 36 shows times to the main heat peak departure obtained from calorimetric measurements at 85ºC for different retarders and cement-to-water ratios of the slurries. The longest setting time was achieved with tartaric acid (TA), while sodium (NaLS, most common retarder) calcium lignosulfonate (CaLS) and sodium salt of polyacrylic acid (PA) also provided some retardation. The longer setting time achieved with PA could be partially the result of higher water demand with this retarder. With the higher water content sodium meta-silicate concentration in solution is lower, which decreases slurries pH and slows down hydration and pozzolanic reactions resulting in longer setting times. Increased water content of the slurries is one of the strategies employed for slowing solidification of fast-setting chemical calcium-phosphate cement. Citric acid was not effective in extending cement setting time. LS acted as a dispersant when combined with TA. The two tested TAs differed in their steric structure (D-(-) and L-(+)), the "new" D-(-)-tartaric acid also being

more economical. This TA provided slightly longer setting time than the "old" (L-(+))one. This, however, could be also due to slightly higher water content in the samples with the "new" TA. Based on these data a combination of "new", more economical, TA with NaLS (LS from now on) was tested for TSRC retardation at different TA/LS ratios with the constant total retarder concentration of 1.5% by weight of cement blend (by the total CAC+FAF content). A very long setting time of more than 70 hours was achieved for TA/LS ratio of 2.5 (Figure 36).
Additional tests performed with a combination of TA and PA did not show any improvement in TSRC retardation. A combination of a common NaLS retarder with TA was recommended for testing to CUDD Energy.
CUDD Energy tested thickening time of TSRC with 1.5% TA/LS (2.5 ratio) at 100°C. A very long thickening time of 16 hours was achieved in the test.

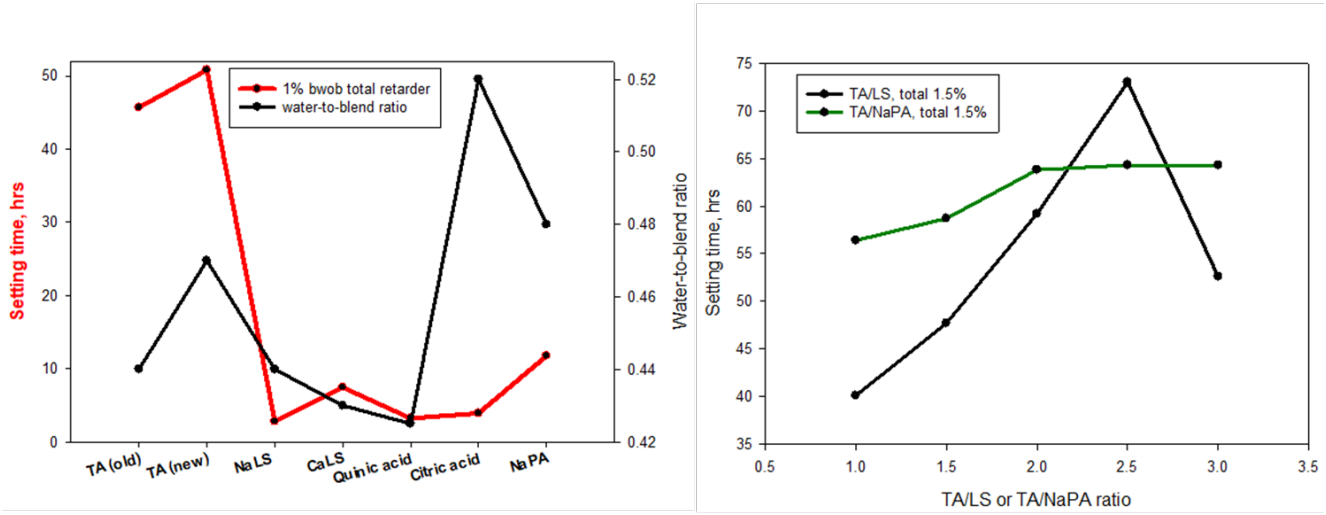

Figure 36. Time to the point of departure (setting time) of the major heat-release peak in calorimetry tests (85°C) for TSRC with different retarders. TA-tartaric acid, NaLS and CaLS – sodium and calcium lignosulfonates, NaPA – sodium polyacrylic acid.

Additional retardation tests were done with "new" TA in combination with another retarder combinations and concentrations (Figure 37). We tested a combination of TA with different known retarders and molecules that potentially could temporarily bind SMS to slow down cement set. Figure 37 shows the effect of different retarder combinations on the time of point of departure (POD) of the major heat release peak, or "set time". The bars of yellow color correspond to the 1% by weight of TSRC total retarder concentration, green ones to 1.3% total retarder concentration, and the blue ones to 1.5% total retarder concentration. For 1% total retarder concentration, ~14% of TA was replaced with either sodium lignosulfonate (NaLS), calcium lignosulfonate (CaLS), polystyrene-maleic acid co-polymer (PSMA), or a combination of CaLS and PSMA. The (CaLS and TA) combination demonstrated the best retardation with the longest POD time of nearly 34 h, the next best solution was replacing 14% of TA with PSMA (28 h) vs. 22 h to POD for TA alone.
In the next series of tests, a third retarder was added to the 1% of TA and NaLS blend at 0.3% by weight of TSRC blend. Addition of citric acid, carboxymethyl cellulose (CMC, MW 2000), and EDTA accelerated POD. Higher MW CMC did not have a strong effect (a small extension of POD time is probably due to the increased water demand of that blend), while urea, CaLS, and PSMA extended the POD time to 22, 42 and 39 h respectively.

In the next series of tests, the total retarder concentration was between 1 and 1.5% by weight of the TSRC blend. Boric acid (BA) and urea were tested in combination with TA and NaLS or TA and CaLS (Figure 37). A combination of urea, TA and CaLS gave the longest time of 42 h followed by the BA, TA and NaLS (36 h). The BA with TA and CaLS showed 34 h to the POD time.
Based on these results it was decided to use a combination of TA with CaLS and test various concentrations of BA as a more economic retarder with this combination. It should be noted that the addition of lignosulfonate helped not only to extend the POD time but also to decrease the intensity of the heat release in the beginning of the tests. This heat release is likely accompanied by the slurry gelation that is very undesirable during the pumping process.
Figure 38 shows the effect of BA concentration on the POD time for TSRC slurry retarded with 1% of TA and CaLS blend. There is no doubt that BA can significantly extend the time to POD in combination with the TA and CaLS. More than 160 h POD time was achieved with 2% BA in the blend.

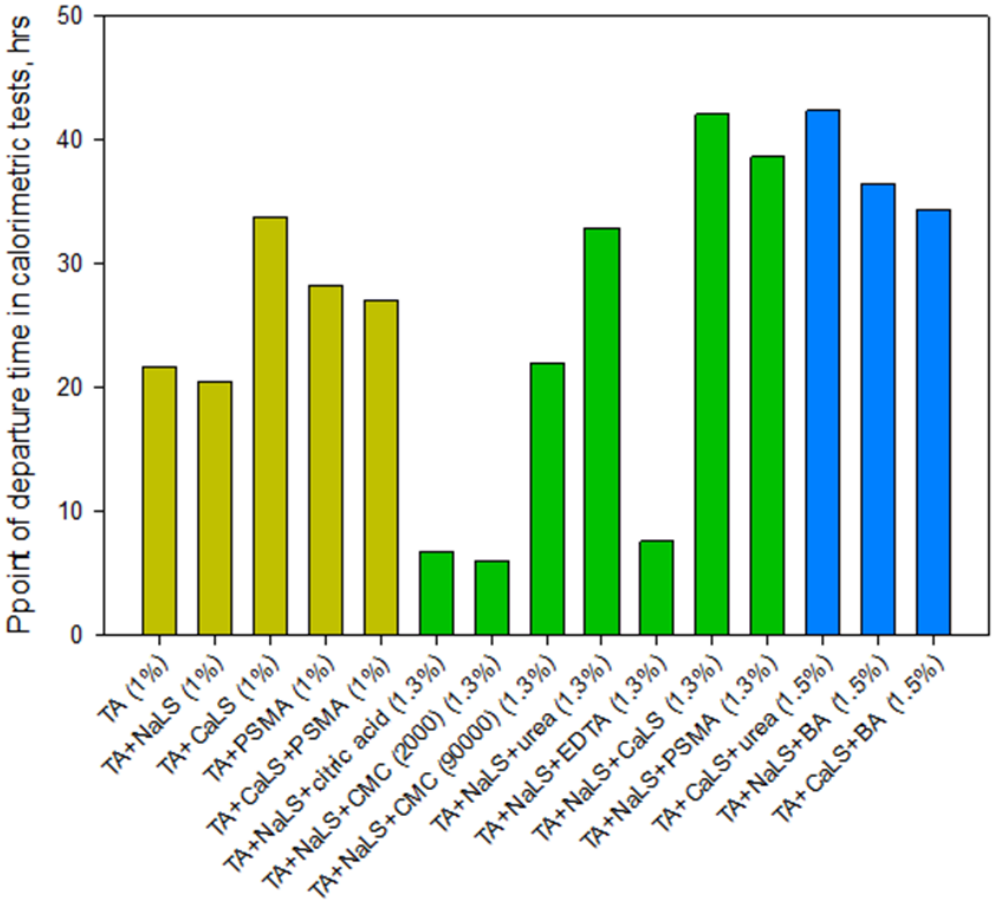

Figure 37. Time to the point of departure (setting time) of the major heat-release peak in calorimetry tests (85ºC) for TSRC with different retarders.

To further extend the setting time of TSRC effect of the SMS concentration in the TSRC blend on the POD time was investigated (Figure 39). These tests were performed on slurries prepared in a small Warring blender under high shear conditions that would correspond to the slurry preparation

in API tests. The data showed that POD time nearly doubles when SMS is decreased to 4 %. With further SMS concentration decrease to 3 and 2% the POD time decreases from more than 60 h at 3% to about 48 h at 2%. These results suggest the optimal concentration of the SMS for the long time to the POD to be around 3-4%.

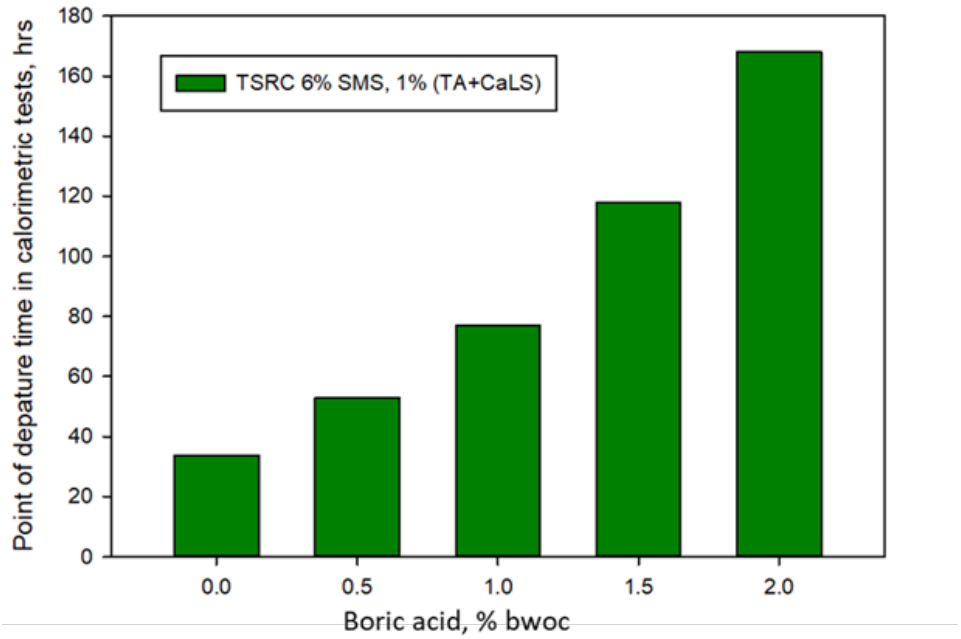

Figure 38. Time to the point of departure (setting time) of the major heat-release peak in calorimetry tests (85°C) for TSRC retarded with 1% TA/CaLS blend and different boric acid concentrations.

We further investigated whether decrease of the SMS content may negatively affect performance of TSRC in thermal shock (TS) as well as its mechanical properties.
Figure 39 presents calorimetric curves of TSRC with different SMS concentrations, and Table 11 shows results of mechanical tests for TSRC blends with different SMS concentrations. The best performance among the tested blends was obtained for the 3% SMS concentration. In fact, a decrease in SMS seemed to be beneficial for the general blend performance.
Figure 40 illustrates the appearance of the metal tubes after the sheath shear bond strength tests for two SMS concentrations. The stronger bond of 3% SMS formulation results in better metal coverage after the casing tube is pushed out of the cement body. The failure takes place in the cement matrix in a cohesive mode. This is desirable since even after the bond failure cement will protect the casing from corrosion. The 3 cycles of thermal shock tests were performed on 300°C cured samples of carbon steel tube with cement sheath. In each cycle the samples were heated to 250°C for 24 hours and then cold water was run through the tube for 10 minutes.
Additional calorimetric tests demonstrated that a sample of TSRC with 3% SMS, retarded by 1% (TA and CaLS) combination with 1.5% by weight of cement boric acid did not set after 9 days at 85°C.
All the results were transferred to CUDD Energy Services for further optimization of the retarder in API tests. Based on the BNL recommendations CUDD Energy ran more than 200 evaluation tests with the TSRC blend. The company did not share all the test results with BNL. The results

reported to BNL show more than 11h of thickening time at 50ºC in API tests at low retarder concentration of 2.2% by weight of blend. The data also show good rheological properties with zero free fluid and low gel strength, indicating stable slurry.
As the result of the tests the company reported that they are confident to retard TSRC blend for any HT geothermal applications.

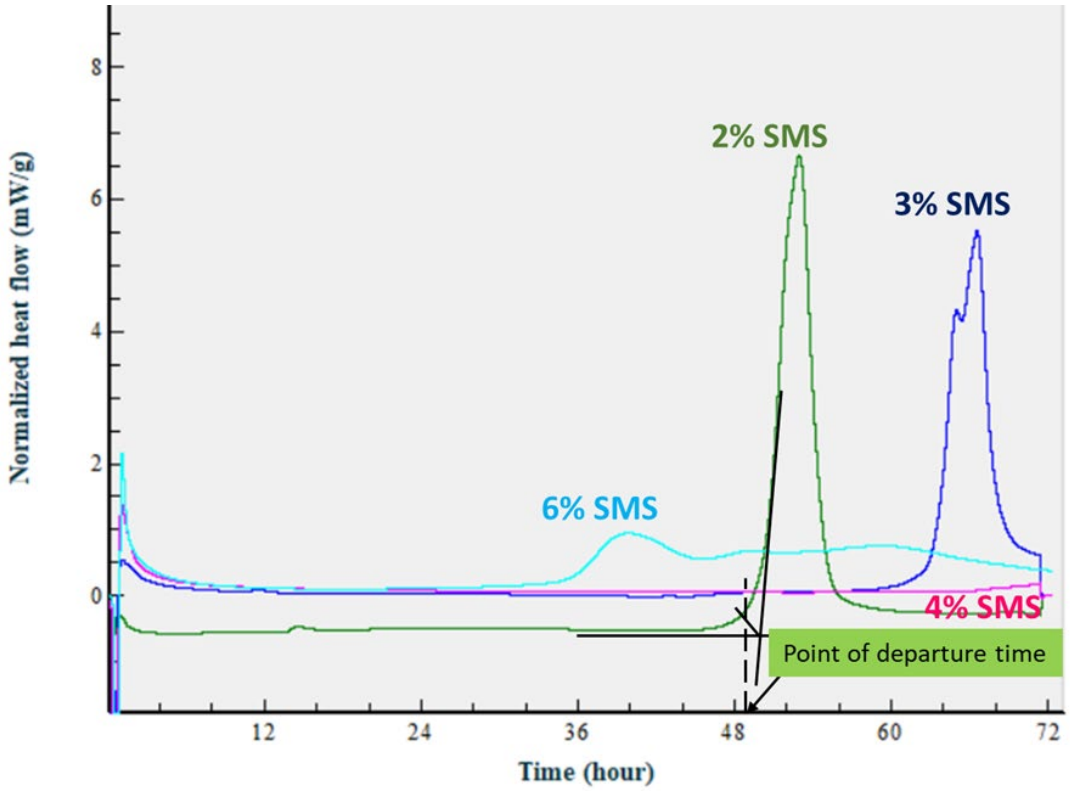

Figure 39. Calorimetric curves of TSRC with different SMS concentrations.

Table 10. Mechanical properties of TSRC with difference concentrations of SMS activator.

Property	**6% SMS**	**3% SMS**	**2% SMS**
Compressive strength, psi (before TS/after TS), psi	1235±40/1415±370	1620±200/1980±140	1730±120/1600±210
Young's modulus (before TS/after TS), kpsi	168±40/172±64	163±92/210±74	190±28/194±40
Compressive toughness (before TS/after TS), N mm/mm^3	0.28±0.08/0.15±0.1	0.36±0.08/0.25±0.04	0.24±0.1/0.25±0.1
Sheath bond strength (before TS/after TS), psi	38±5/13±1	NA	86±6/67±14

Figure 40. Appearance of carbon steel tubes after the shear-bond tests for TSRC samples with 3 and 6% SMS concentrations before and after the thermal shock tests.

2.4.Work on the consistency of the blend performance and simplified field logistics

In the frame of the project, we evaluated consistency of the TSRC blend performance with different batches of fly ash F and how logistics of CAC-based blend field applications can be simplified by using a special grade of CAC, which is more compatible with OPC. MK, perlite, and CAC, grade PP8172 (PP) were provided by Imerys, FAF-batch2 was received from CUDD Energy Services. Mechanical properties of the reference blend and TSRC blend with various substitutions are given in Figures 41 and 42.

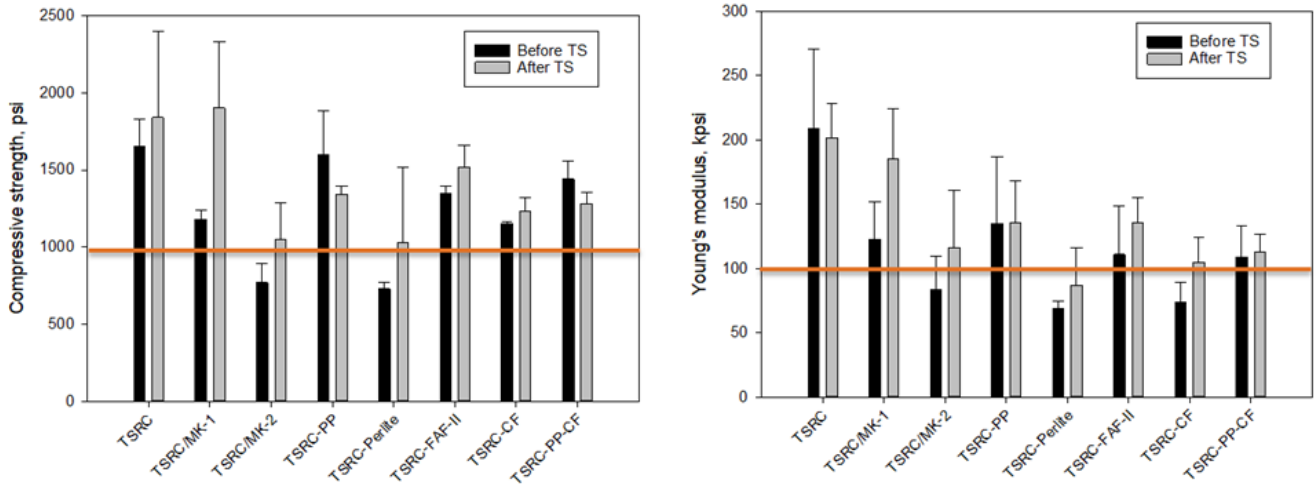

Figure 41. The compressive strength and Young's modulus of the reference TSRC blend and TSRC blends with FAF-batch1 replaced with MK at different concentrations, FAF-batch2, perlite; TSRC re-enforced with carbon fibers (CF), or TSRC with CAC#80 replaced by a special CAC grade (PP) more compatible with OPC. TSRC-1: #80/MK/Silica flour-60/20/20; TSRC-2: #80/MK/27/3.

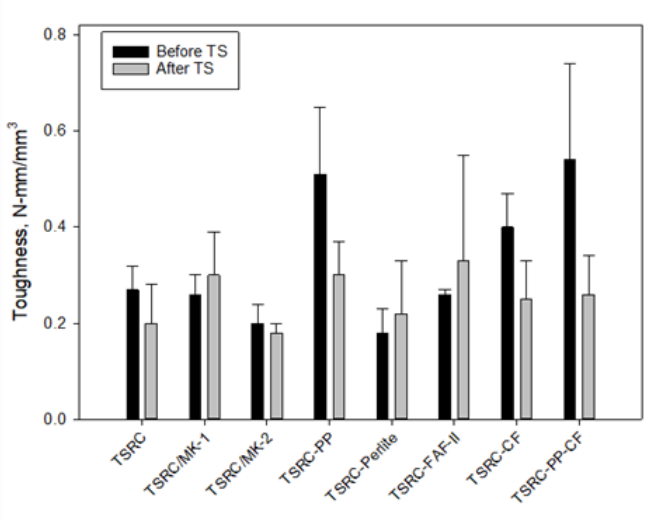

Figure 42 The toughness of the reference TSRC blend and TSRC blends with FAF-batch1 replaced with MK at different concentrations, FAF-batch2, perlite; TSRC re-enforced with carbon fibers (CF), or TSRC with CAC#80 replaced by a special CAC grade (PP) more compatible with OPC.

Since FAF is a by-product, it has a variable composition that potentially can affect performance of the TSRC blend. Discussion with CUDD Energy services helped to establish that significant changes in performance of FAF are related to variations in calcium content in it. These in turn occur after rain. The reason is the use of lime by power plants to spread on coal in humid weather. We tested mechanical properties of the blend with two different types of FAF and possible well-defined FAF substitutions – perlite and MK. Perlite is a lightweight product that produces lower density cement than fly ash (11 vs. 13 ppg), which necessarily results in lower strength cement. The blends were autoclaved for a day at 300ºC and then subjected to 3 thermal shock cycles where in each cycle, cements were heated to 400ºC for 24 hours and then placed into water at 25ºC.
All the substitutions performed well under the thermal shock conditions. The reference blend showed higher strength and Young's modulus than the blends with the substitutions (Figure 41). However, apart from the blend with perlite and TSRC-2 (#80/MK/Silica flour – 60/27/3) all blends developed compressive strength above 1000 psi after the 300ºC autoclaving. For both blends that did not meet the 1000 psi target the strength increased after the thermal shock cycles, as it did for all other tested blends except the one with the CAC#80 replacement by PP. Although that blend lost some strength in the thermal shock cycling, the strength loss was only 15%. TSRC formulated with PP cement was compatible with carbon fiber reinforcement. The mechanical properties of the reinforced TSRC-PP were in the range of those of the reference blend reinforced with carbon fibers.
The toughness of most of the blends was above that of the reference (Figure 42). Noticeable, the toughness was more than 60% higher for the blend with #80 replacement. For most of the blends the toughness predictably decreased after the thermal shock cycling due to the increase of cement brittleness, but it remained within the range of the reference blend's toughness.
In summary, TSRC blend can be formulated with cement providing better compatibility with OPC if needed, and FAF can be replaced with silica, MK, perlite (for cements with lower density). TSRC performance was not highly sensitive to different FAF batches.

3. CONCLUSIONS

The project focused on four major topics: 1) advancing Thermal-Shock-Resistant cement (TSRC) to geothermal field applications through the development and evaluation of its field applicable formulation in collaboration with a service company (CUDD Energy Services); 2) confirming consistence of TSRC performance with variations of blends composition (replacing fly ash F (FAF) with other aluminum-silica materials and testing its performance with different FAF batches); 3) simplifying logistics of the blend use by using calcium-aluminate cement (CAC) that is more compatible with OPC in its composition; 4) confirming performance of advanced cement blends vs. OPC-based blends in deep, hot geothermal environment (Newberry well, Oregon, US).

The project achieved all its goals. Performance of TSRC was validated with metakaolin (MK) or perlite substitutions of FAF and a different FAF batch in mechanical properties tests and thermal cycling. The possibility of replacing CAC #80 in TSRC composition with more OPC-friendly CAC PP8172 was demonstrated at 300ºC and temperature cycling tests. The results showed robustness of TSRC formulations to composition changes. The thickening (setting) time of TSRC for pumpability into deep geothermal wells was successfully extended in collaboration with CUDD Energy Services. The blend solidification can be retarded for any deep-well placement at high temperatures (HT) according to the service company.
Most importantly, the field-exposure tests clearly demonstrated that currently used OPC-based cement blends are not stable under HT geothermal conditions. While mechanical properties of all formulations rich in aluminum tested in the field exposure tests persisted throughout the trial of 9 months, OPC/silica blend lost more than 80% of its strength. The composition analyses showed that the blend was severely carbonated, the major crystalline phase, xonotlite, transformed into calcium (bi)carbonate. This phase transition occurred over time with the initial blend carbonation resulting in enhanced mechanical properties after 3 months of exposure followed by complete cement degradation after only 9 months of the well exposure tests. The project decisively showed that OPC-based cements are not stable under the HT geothermal conditions, as well as the advantage of Al-rich formulations, including TSRC, for such applications.

4. ACKNOWLEDGEMENTS

This work was supported by the Geothermal Technologies Office in the US Department of Energy (DOE) Office of Energy Efficiency and Renewable Energy (EERE), under the auspices of the US DOE, Washington, DC, USA, under contract No. DE-AC02-98CH 10886.
This research was partially funded by the Geothermica project “Sustainable Geothermal Well Cements for Challenging Thermo-Mechanical Conditions (TEST-CEM)”, number 2003184001. The project has been subsidized through the Cofund GEOTHERMICA by DoE (the USA), RVO NL (The Netherlands), and the Research Council of Norway.
Research was carried out in part at the Center for Functional Nanomaterials, Brookhaven National Laboratory, which is supported by the US Department of Energy, Office of Basic Energy Sciences, under contract No. DE-SC0012704.

5. REFERENCES

Chatterjee, N. D. (1970). Synthesis and Upper Stability of Paragonite*. In *Contr. Mineral. and Petrol* (Vol. 27).

Christidis, G. E. (2011). Industrial clays. In *European Mineralogical Union Notes in Mineralogy* (Vol. 9, Issue 1, pp. 341–414). Universitat Jena - Mineralogie. https://doi.org/10.1180/EMU-notes.9.9

Cruciani, G. (2006). Zeolites upon heating: Factors governing their thermal stability and structural changes. *Journal of Physics and Chemistry of Solids*, *67*(9–10), 1973–1994. https://doi.org/10.1016/j.jpcs.2006.05.057

Dai, X., Aydin, S., Yardimci, M. Y., Lesage, K., & de Schutter, G. (2020). Influence of water to binder ratio on the rheology and structural Build-up of Alkali-Activated Slag/Fly ash mixtures. *Construction and Building Materials*, *264*. https://doi.org/10.1016/J.CONBUILDMAT.2020.120253

Drüppel, K., & Wirth, R. (2018). Metasomatic replacement of albite in nature and experiments. *Minerals*, *8*(5). https://doi.org/10.3390/min8050214

Feng, D., Provis, J. L., & Van Deventer, J. S. J. (2012). Thermal activation of albite for the synthesis of one-part mix geopolymers. *Journal of the American Ceramic Society*, *95*(2), 565–572. https://doi.org/10.1111/j.1551-2916.2011.04925.x

Fischer, S., Zemke, K., Liebscher, A., & Wandrey, M. (2011). Petrophysical and petrochemical effects of long-term CO2- exposure experiments on brine-saturated reservoir sandstone. *Energy Procedia*, *4*, 4487–4494. https://doi.org/10.1016/j.egypro.2011.02.404

Foldvari, M. (2011). *Handbook of thermogravimetric system of minerals and its use in geological practice*. Geological institute of Hugary.

Gill, S. K., Pyatina, T., & Sugama, T. (2012). Thermal shock-resistant cement. *Transactions - Geothermal Resources Council*, *36 1*.

Kamath, M., Prashant, S., & Kumar, M. (2021). Micro-characterisation of alkali activated paste with fly ash-GGBS-metakaolin binder system with ambient setting characteristics. *Construction and Building Materials*, *277*. https://doi.org/10.1016/J.CONBUILDMAT.2021.122323

Li, L., Xie, J., Zhang, B., Feng, Y., & Yang, J. (2023). A state-of-the-art review on the setting behaviours of ground granulated blast furnace slag- and metakaolin-based alkali-activated materials. *Construction and Building Materials*, *368*(October 2022), 130389. https://doi.org/10.1016/j.conbuildmat.2023.130389

Liu, H., Sanjayan, J. G., & Bu, Y. (2017). The application of sodium hydroxide and anhydrous borax as composite activator of class F fly ash for extending setting time. *Fuel*, *206*, 534–540. https://doi.org/10.1016/J.FUEL.2017.06.049

Mac, F., Diego, O., Hollman, N., Javier, U., Alberto, G., Brothers, L., & Herman, P. (2014). Long-term calcium phosphate cement for in-situ combustion project. *Society of Petroleum Engineers - SPE Heavy Oil Conference Canada 2014*, *1*, 216–225. https://doi.org/10.2118/170016-ms

Meng, M., Pyatina, T., Frash, L., Bijay, K., Madenova, Y., Uwaila, I., & Zhang, W. (2024). Mechanical Performance of One Latex Cement System for Thermal Storage Wells. *ARMA 24-248, 58th US Rock Mechanics/Geomechanics Symposium*.

Munz, I. A., Brandvoll, Haug, T. A., Iden, K., Smeets, R., Kihle, J., & Johansen, H. (2012). Mechanisms and rates of plagioclase carbonation reactions. *Geochimica et Cosmochimica Acta*, *77*, 27–51. https://doi.org/10.1016/j.gca.2011.10.036

Murakami, T., Kogure, T., Kadohara, H., & Ohnuki, T. (1998). Formation of secondary minerals and its effect on anorthite dissolution. In *American Mineralogist* (Vol. 83).

Oelkers, E., Gislason, S. R., & Matter, J. (2008). Mineral Carbonation of CO2. *Elements*, *4*(5), 333–337.

Pyatina, T., & Sugama, T. (2018). Cements for High-Temperature Geothermal Wells. In *Cement based materials* (IntechOpen, pp. 221–235).

Pyatina, T., & Sugama, T. (2019a). Self-healing and crack-sealing ability of 30-day-long 300oC cured Thermal Shock Resistant Cement composites. *GRC Transactions*, *43*.

Pyatina, T., & Sugama, T. (2019b). Thermal Shock Resistant Cement for heat storage. *GRC Transactions*, *43*.

Pyatina, T., & Sugama, T. (2023). Cements for Supercritical Geothermal Wells at 400oC. *GRC Transactions, Vol. 47*, 447–467.

Pyatina, T., Sugama, T., Moghadam, A., Naumann, M., Skorpa, R., Feneuil, B., Soustelle, V., & Godøy, R. (2024). Assessment of Cementitious Composites for High-Temperature Geothermal Wells. *Materials*, *17*(6). https://doi.org/10.3390/ma17061320

Pyatina, T., Sugama, T., Moon, J., & James, S. (2016). Effect of tartaric acid on hydration of a sodium-metasilicate-activated blend of calcium aluminate cement and fly ash F. *Materials*, *9*(6). https://doi.org/10.3390/ma9060422

Sugama, T., Carciello, N. R., Nayberg, T. M., & Brothers, L. (1995). Mullite Microspher-filled Lightweight Calcium Phosphate Cement Slurries for Geothermal Wells: Setting and Properties. *Cement & Concrete Research*, *25*(6), 1305–1310.

Sugama, T., & Pyatina, T. (2015). Effect of sodium carboxymethyl celluloses on water-catalyzed self-degradation of 200 °c-heated alkali-activated cement. *Cement and Concrete Composites*, *55*. https://doi.org/10.1016/j.cemconcomp.2014.09.015

Sugama, T., & Pyatina, T. (2018). *Alkali-activated cement composites for high temperature geothermal wells*. Scientific Research Books.

Sugama, T., & Pyatina, T. (2019). Self-healing, re-adhering, and corrosion-mitigating inorganic cement composites for geothermal wells at 270-300degC. *BNL-2019-IR*.

Sugama, T., & Pyatina, T. (2021). Hydrophobic Lightweight Cement with Thermal Shock Resistance and Thermal Insulating Properties for Energy-Storage Geothermal Well Systems. *Materials*, *14*, 6679.

Sugama, T., & Pyatina, T. (2022, February 7). Cement Formulations for Super-Critical Geothermal Wells. *47th Workshop on Geothermal Reservoir Engineering*.

Taylor, H. F. W. (1997). *Cement Chemistry* (2nd ed.). Thomas Telford Publishing.

Thorbjornsson, I., & Kaldal, G. (2021). *Flexible Couplings for Improved Casing Design in High-Temperature Geothermal Wells*.

Tong, S., Yuqi, Z., & Qiang, W. (2021). Recent advances in chemical admixtures for improving the workability of alkali-activated slag-based material systems.

Construction and Building Materials, *272*. https://doi.org/10.1016/J.CONBUILDMAT.2020.121647

Weber, E., Emerson, E., Harris, K., & Brothers, L. (1998). The Application of a New Corrosion Resistant Cement in Geothermal Wells. *Geothermal Resource Council Transactions*, *22*, 25–30.

Interdisciplinary Sciences Department
Building # 734
P.O. Box 5000
Upton, NY 11973-5000

www.bnl.gov